Numerical Sampling of Nonadiabatic Dynamics of Quantum-Classical Systems

---

by

Daniel A. Uken

Submitted in fulfilment of the

requirements for the degree of

Master of Science

in the

School of Physics

University of KwaZulu-Natal

Pietermaritzburg

November 2010

As the candidate's supervisor I have approved this dissertation for submission.

Signed:　　　　　　　　Name: Dr. A. Sergi　　　　Date:

Abstract

The simulation of the dynamics of quantum systems is very difficult, due to the fact that, in general, it cannot be calculated exactly for interacting many-body systems. Brute force simulations of quantum dynamics are simply not feasible, and approximations need to be made. In many instances a quantum system can be approximated as a quantum-classical system, where only a subsystem of interest is treated quantum mechanically, and the rest is considered as a classical bath. When energy is free to be exchanged between the subsystem and its environment, the dynamics that occur is said to be nonadiabatic. This type of dynamics is challenging to calculate on a computer, as it can lead to large statistical errors at long times. Hence, there is a need for improved algorithms for nonadiabatic dynamics. In this thesis, a recently introduced nonadiabatic sampling scheme [A. Sergi and F. Petruccione, Phys. Rev. E **81**, 032101 (2010)] is used to calculate the long-time dynamics of a model system comprising a quantum spin coupled to a bath of harmonic oscillators. Also, various technical aspects of the algorithm are investigated.

Preface

The computational work described in this dissertation was carried out in the School of Physics, University of KwaZulu-Natal, Pietermaritzburg, from January 2010 to October 2010, under the supervision of Doctor Alessandro Sergi.

These studies represent original work by the author and have not otherwise been submitted in any form for any degree or diploma to any tertiary institution. Where use has been made of the work of others it is duly acknowledged in the text.

Declaration 1 - Plagiarism

I, ... declare that

- The research reported in this thesis, except where otherwise indicated, is my original research.

- This thesis has not been submitted for any degree or examination at any other university.

- This thesis does not contain other persons data, pictures, graphs or other information, unless specifically acknowledged as being sourced from other persons.

- This thesis does not contain other persons' writing, unless specifically acknowledged as being sourced from other researchers. Where other written sources have been quoted, then:

  a. Their words have been re-written but the general information attributed to them has been referenced

  b. Where their exact words have been used, then their writing has been placed in italics and inside quotation marks, and referenced.

- This thesis does not contain text, graphics or tables copied and pasted from the Internet, unless specifically acknowledged, and the source being detailed in the thesis and in the Bibliography.

Signed: ....

Declaration 2 - Publications

Details of contribution to publications that form part and/or include research presented in this thesis:

Publication 1 - D. A. Uken, A. Sergi and F. Petruccione, "Stochastic Simulation of Nonadiabatic Dynamics at Long Time", arXiv:1003.31172 [quant-ph] (2010)

Status: Submitted to and accepted by *Physica Scripta*

Computational work performed by D. A. Uken, paper written mostly by A. Sergi, in part by D. A. Uken. Work performed in collaboration with F. Petruccione.

Publication 2 - D. A. Uken and A. Sergi, "Momentum Shift in Nonadiabatic Dynamics"

Status: Submitted to *Modern Physics Letters B*

Computational work performed by D. A. Uken, paper written mostly by A. Sergi, in part by D. A. Uken.

Signed: ....

Contents

Acknowledgements

I would like to begin by thanking my supervisor, Dr. Alessandro Sergi, for his assistance in understanding the theory and always keeping me motivated to give of my best. His constant enthusiasm for our work and long philosophical conversations throughout the year have inspired my great interest in my line of study.

Secondly, to my parents, brother Philip, sister Paula and girlfriend Paula, for their understanding during the months of late nights and for always supporting me in my studies. Without their care I would not have been able to accomplish what I have.

Finally, I would like to acknowledge the National Institute for Theoretical Physics (NITheP) for the bursary they awarded me, without which I would not have been able to complete my MSc in Physics.

Chapter 1

Introduction

While quantum theory has been well known for almost a century, one of the greatest problems encountered by computational physicists today remains the development of algorithms for calculating the dynamics of quantum systems. This difficulty stems from the theory itself; indeed, for most many-body quantum systems their dynamics is unsolvable, and approximations have to be made to obtain solutions.

When solving classical dynamics of many-body systems numerically, there a number of algorithms which are very general, and can be used to simulate a wide range of different systems. Most commonly, Molecular Dynamics, or Monte Carlo methods are used for classical dynamics [1]. Classical theory, however, is given in terms of functions of phase-space, which are suited to implementation on a computer. Quantum theory is rather more complex, since it is defined in terms of operators which may or may not commute. This is what causes quantum dynamics to be so difficult to simulate. Unlike classical dynamics, there is no general algorithm or method for solving the dynamics of quantum systems. Algorithms are generally tailored specifically for the system or problem of study.

An additional problem which is very limiting on numerical quantum dynamics is simply that, in many cases, the required computer memory far

exceeds that which is available. In [1] it is shown that even for a lattice of as few as 64 electrons, the memory that is required to solve the system completely is of the order of 10^{28}Gb, which is obviously completely unfeasible.

To construct any successful algorithm for simulating quantum dynamics, one of the main objectives will be to reduce the computational resources required for the calculation. It is pointless to devise a simulation scheme that can solve a quantum system accurately if there is no computer capable of running it. It is also obviously desirable for any simulation to complete in a reasonable length of time.

Good quantum algorithms therefore generally rely on making approximations which, while dramatically reducing run-time and system resources, do not sacrifice the integrity of the result. A highly useful approximation is that of quantum-classical dynamics [2, 3]. When studying a quantum system, there is often a subsystem of interest which is interacting with its environment. In the quantum-classical approximation, only the subsystem is considered as being quantum, and the environment is treated in a classical way. This greatly simplifies the algorithm required to simulate the dynamics, since classical dynamics is so well studied and so much easier to calculate numerically. Many systems can be approximated this way, either because the degrees of freedom of the environment are numerous enough to be approximated as classical, or because it is not required to know the detailed evolution of the bath to obtain good results for the quantum subsystem. Because so many systems can be approximated as quantum-classical, the numerical study of quantum-classical dynamics is of interest in a wide range of topics.

Quantum information processing [4, 5] - a relatively new field which concerns using quantum principles in an effort to achieve greater capabilities of information processing and transfer - utilises many systems that can be treated semiclassically. Aspects such as external control in quantum optics

[6, 7], quantum transport through meso- and nanoscale structures, quantum tunneling in macroscopic systems, and quantum Brownian motors, all relate to dissipative quantum systems which can be treated semiclassically [8]. Dynamical properties of such systems can be calculated using a quantum-classical formalism. It has also been demonstrated that rate constants of chemical reactions and transport coefficients can computed using a quantum-classical approach [9].

There is a further problem to simulating dynamics, however, even in the quantum-classical approximation. When a subsystem of interest and the classical bath are free to exchange energy, the dynamics is said to be nonadiabatic. If no energy is exchanged, then the dynamics is adiabatic. Adiabatic dynamics of quantum-classical systems is relatively easy to formulate, as evolution occurs on one potential energy surface. It is more complicated, however, to model nonadiabatic dynamics. The implementation of nonadiabatic quantum transitions between potential energy surfaces is difficult to achieve computationally, and so approximations have to be made. In general, the implementation of nonadiabatic transitions is performed in a stochastic way, using sampling probabilities. However, these algorithms result in large statistical error in the calculation after long time intervals, so that meaningful results can only be obtained for short times. Recently, an improved sampling probability was proposed, which reduced this long-time error, allowing good results to be achieved for greater times [10].

The nature of the equations of motion for mixed quantum-classical systems are not clear, since the interaction between the bath and quantum subsystem results in the bath acquiring certain quantum-like characteristics [2]. If stationary phase analysis of the equations of motion is performed, it can be shown that the variational principle giving the equations of motion is non-Lagrangian in nature, and the equations do not result in unique solutions [11]. There are various methods for solving mixed quantum-

classical dynamics. One of the most common strategies for dealing with quantum-classical systems is to devise a so-called surface-hopping scheme [12-16]. Surface-hopping algorithms describe quantum-classical dynamics as adiabatic evolution on potential energy surfaces interspersed by nonadiabatic transitions to different energy surfaces. One of the more recent surface-hopping schemes is based on the quantum-classical Liouville equation [17, 18, 19, 20, 21, 22, 23, 24]. This equation results in a formulation which realises the statistical mechanics of quantum-classical dynamics in terms of a density matrix. In a convenient basis, this formulation leads naturally to the development of surface-hopping schemes due to the way in which the evolution can be separated into adiabatic and nonadiabatic parts, where the latter are generally realised by a transition operator.

In part of the research reported here, an existing surface-hopping algorithm has been used, together with the improved transition sampling scheme in [10]. Calculations were performed for system parameters which have not been presented thus far [25], and it is shown that the statistical error was greatly reduced.

A detailed study of the momentum-jump approximation was also performed. This approximation is used in surface-hopping schemes to realise the action of the transition operator on the classical bath, by shifting bath momenta. The effects of three different momentum-shift rules [26] were examined, in an effort to better understand what properties are important when devising a successful sampling scheme for nonadiabatic transitions.

The layout of the thesis is as follows. Chapter 2 introduces some of the theory used when simulating quantum-classical systems. The Wigner phase-space representation of quantum mechanics is defined, as well as the quantum-classical bracket. In Chapter 3, two common bases used for simulating quantum-classical dynamics are discussed, and the so-called surface hopping algorithms are introduced - specifically, the sequential short-time

propagation algorithm [27], which are used to obtain results. Chapter 4 defines the model used to represent the simulated quantum-classical system, and presents the results of numerical studies, including the study of momentum-jump rules for nonadiabatic transitions and results of calculations using the improved sampling scheme of [10] for system parameters hitherto unshown in literature. Finally, Chapter 5 concludes by discussing the results and their relevance in achieving accurate results for simulations at longer times, as well as possible future work. In the appendices, several aspects of the theory are derived.

Chapter 2

Theory of Quantum-Classical Systems

This chapter discusses, in detail, the theory required to understand and simulate quantum-classical dynamics. It starts with a brief summary of Heisenberg's formulation of quantum mechanics and introduces the density matrix operator. Representation of quantum mechanics in phase-space is examined, in particular, the Wigner representation. This is followed by a general outline of bracket algebra, and concludes by defining the quantum-classical bracket.

2.1 Heisenberg's Formulation of Quantum Mechanics

Formulated in June 1925 by Werner Heisenberg, this was the first full description of quantum mechanics to be developed [28]. Also known as matrix mechanics, this formulation is equivalent to the wave theory of Schrödinger. In Heisenberg theory, operators are represented by matrices that act on quantum states represented by vectors - either column vectors (kets), or row vectors (bras).

The dimensions of these matrices and vectors are governed by the number of basis vectors required to form a complete basis set for the system. If a system can be described by a minimum of N basis states (vectors), then operators for that system are $N \times N$ matrices, kets are $N \times 1$ column vectors, and bras $1 \times N$ row vectors.

One of the main differences between the Heisenberg representation and that of Schrödinger, is the placement of time dependence. Consider a 1D system with state $|\psi\rangle$ at time $t = 0$. In the Schrödinger picture, to calculate the expectation value of an arbitrary operator $\hat{\chi}$ at a future time $t = t'$, the Schrödinger wave equation is used to evaluate the wave function $\psi(x, t')$, and then the expectation value

$$\langle \chi(t') \rangle = \int \psi^*(x, t') \hat{\chi} \psi(x, t') \, dx \; , \tag{2.1}$$

is evaluated. In this representation, the states evolve in time, and the operators are constant. In the Heisenberg picture, the reverse is true. In the same situation as above, the observable would be calculated by determining the operator at the future time, and then acting it upon time independent states. Any operator $\hat{\chi}$ changes in time according to the Heisenberg equation of motion

$$\frac{d\hat{\chi}(t)}{dt} = \frac{i}{\hbar} \left[\hat{H}, \hat{\chi}(t) \right] + \left(\frac{\partial \hat{\chi}}{\partial t} \right) \; , \tag{2.2}$$

where $[\hat{H}, \hat{\chi}(t)] \equiv \hat{H}\hat{\chi}(t) - \hat{\chi}(t)\hat{H}$. Equation (2.2) can, in fact, be derived using Equation (2.1), which is evidence of the fact that the Heisenberg and Schródinger representations are equivalent. This derivation is performed in Appendix A. In (2.2), the operator may have an explicit time dependence. However, from now on, only operators without an explicit time dependence are considered, and the Heisenberg equation of motion simplifies to

$$\frac{d\hat{\chi}(t)}{dt} = \frac{i}{\hbar}\left[\hat{H}, \hat{\chi}(t)\right] . \tag{2.3}$$

2.2 Quantum Statistical Mechanics

In both classical and quantum mechanics, statistical theories are required when the initial conditions for a system are not known. Due to the Heisenberg indeterminacy principle, quantum mechanics has an additional level of uncertainty which gives it an intrinsic statistical nature [29]. Even if quantum states and operators are propagated in time by deterministic equations, the results of these are still only linked to the physical world in a statistical way.

When it can be said with complete certainty that a system is in a specific state $|\psi\rangle$, the system is said to be in a pure state. This state vector can be represented in an orthonormal basis $|\phi_j\rangle$ as

$$|\psi\rangle = \sum_j c_j |\phi_j\rangle , \tag{2.4}$$

where $c_j = \langle\phi_j|\psi\rangle$ are coefficients with $\sum_j |c_j|^2 = 1$. Consider now an operator $\hat{\chi}$ for which $\hat{\chi}|\phi_j\rangle = a_j|\phi_j\rangle$, where a_j is a real number. The average of this operator for a system in pure state $|\psi\rangle$ is given by

$$\bar{\chi} = \langle\psi|\hat{\chi}|\psi\rangle . \tag{2.5}$$

Substituting Eq. (2.4) into Eq. (2.5) gives

$$\begin{aligned}
\hat{\chi} &= \sum_j \sum_k c_j c_k^* \langle\phi_j|\hat{\chi}|\phi_k\rangle \\
&= \sum_j \sum_k c_j c_k^* a_k \langle\phi_j|\phi_k\rangle \\
&= \sum_j \sum_k c_j c_k^* a_k \delta_{jk}
\end{aligned}$$

$$= \sum_k |c_k|^2 a_k \ . \tag{2.6}$$

The last line above demonstrates that even if everything about the initial conditions of the system is known, the measurable quantities are given by statistical averages. This is because the Heisenberg indeterminacy principle gives quantum mechanics a second inherent level uncertainty not encountered in classical mechanics.

2.2.1 The Density Matrix

If a system of interest with coordinates (x) is coupled to an environment with coordinates (y), while it is possible for the entire system to have a wave function $\Psi(x, y)$, it does not necessarily follow that the subsystem with coordinates (x) has its own wave function $\Psi(x)$. This is due to the fact that $\Psi(x, y)$ cannot in general be written as a product of wave functions $\Phi(x)\Phi(y)$ [30].

In this case, it is not possible to know what state the subsystem of interest is in, it is only possible to know the probabilities that the subsystem is in each accessible microstate. It is convenient to introduce a statistical ensemble of identical systems, and the probabilities then give the fraction of the ensemble in each microstate.

Since not all the systems in the ensemble are in the same state, averages of observables can no longer be calculated according to Equation (2.6). Averages for the ensemble must now be calculated by determining the average for each accessible state, and summing all the terms, each weighted by the probability associated with that state [29]:

$$\begin{aligned}
\langle \hat{\chi} \rangle &= \sum_i \gamma_i \bar{\chi}_i \\
&= \sum_i \gamma_i \sum_j \sum_k c_j^{i*} c_k^i \langle j|\hat{\chi}|k \rangle \ ,
\end{aligned} \tag{2.7}$$

where γ_i is the probability that the system is in the state $\Psi^i(x)$. These probabilities are all positive, and must satisfy the normalisation condition

$$\sum_i \gamma_i = 1 \ . \tag{2.8}$$

Using Eq. (2.7), it is now possible to introduce the matrix element

$$\rho_{kj} \quad = \quad \sum_i \gamma_i c_k^i c_j^{i*} \ , \tag{2.9}$$

in terms of which

$$\langle \chi \rangle = \sum_j \sum_k \chi_{jk} \rho_{kj} \ . \tag{2.10}$$

The operator $\hat{\rho}$ can now be defined, with matrix elements ρ_{kj}. This operator is known as the von Neumann density matrix [29]. It follows from the definition for the matrix elements in Equation (2.8) that $\hat{\rho}$ is a Hermitian operator, since

$$
\begin{aligned}
(\rho_{kj})^* \quad &= \quad \left(\sum_i \gamma_i c_k^i c_j^{i*} \right)^* \\
&= \quad \sum_i \gamma_i c_k^{i*} c_j^i = \rho_{jk} \ .
\end{aligned}
\tag{2.11}
$$

The matrix elements may also be written in terms of the bra-ket notation as

$$\rho_{kj} = \langle k | \hat{\rho} | j \rangle \ . \tag{2.12}$$

Using this form for the matrix elements, it is apparent that the average $\langle \hat{\chi} \rangle$ in Eq. (2.9) is given in terms of a product of operators:

$$\langle \hat{\chi} \rangle \quad = \quad \sum_j \sum_k \langle j | \hat{\chi} | k \rangle \langle k | \hat{\rho} | j \rangle$$

$$= \sum_j \langle j|\hat{\chi}\hat{\rho}|j\rangle \; , \qquad\qquad (2.13)$$

where the closure relation has been used. Equation (2.13) gives the average as the sum of the diagonal matrix elements of the matrix product of $\hat{\chi}$ and $\hat{\rho}$, that is, the trace. Since the trace of a matrix is basis-independent, the identity $Tr(AB) = Tr(BA)$ can be used, and the observable can be written in general form

$$\langle\hat{\chi}\rangle = Tr\,\hat{\chi}\hat{\rho} = Tr\,\hat{\rho}\hat{\chi} \; . \qquad\qquad (2.14)$$

It follows from Eqs. (2.8) and (2.9) that the trace of the density matrix must be unity:

$$
\begin{aligned}
Tr\,\hat{\rho} &= \sum_j \rho_{jj} \\
&= \sum_i \gamma_i \sum_j |c_j^i|^2 \\
&= \sum_i \gamma_i = 1 \; . \qquad\qquad (2.15)
\end{aligned}
$$

The diagonal elements of the density matrix are thus the fractional populations of the ensemble for each accessible state. This leads to another useful property of the density matrix. For a pure state, one of the γ_i will be equal to 1, with all the others zero, and therefore

$$Tr\,(\hat{\rho}^2) = 1 \; . \qquad\qquad (2.16)$$

For a mixed state, this will naturally not be the case, since more than one γ_i will be non-zero.

While this normalised property of the diagonal elements of $\hat{\rho}$ applies in any basis, there are no intrinsic properties of the off-diagonal elements. A density matrix may be diagonal in one basis, but it does not mean it is diagonal in another basis. Furthermore, unlike the diagonal elements, the

off-diagonal elements may be either positive or negative. These elements are related to the coherence effects in a system, and are a consequence of the wave-like properties of matter [29].

Just as the wave function has an equation of motion in the Schrödinger equation, so does the density matrix in the von Neumann equation obtained below. Consider the average for the operator $\hat{\chi}$ at some time t:

$$
\begin{aligned}
\langle \chi(t) \rangle &= Tr \ (\hat{\chi}(t)\hat{\rho}) \\
&= Tr \ \left(e^{i\hat{H}t/\hbar} \hat{\chi} e^{-i\hat{H}t/\hbar} \hat{\rho} \right) \ ,
\end{aligned} \tag{2.17}
$$

where $\hat{H}$ is time independent. Exploiting the cyclic invariance of the trace, this becomes

$$
\begin{aligned}
\langle \chi(t) \rangle &= Tr \ \left(\hat{\chi} e^{-i\hat{H}t/\hbar} \hat{\rho} e^{i\hat{H}t/\hbar} \right) \\
&= Tr \ (\hat{\chi}\hat{\rho}(t)) \ ,
\end{aligned} \tag{2.18}
$$

where the time dependence of the density matrix is defined in the last line. Equation (2.17) can be thought of as the Heisenberg picture of quantum statistical mechanics, while Eq. (2.18) represents that of Schrödinger. The von Neumann equation of motion for the density matrix can be obtained by

$$
\begin{aligned}
\frac{\partial}{\partial t}\hat{\rho}(t) &= \frac{\partial}{\partial t}\left[e^{-i\hat{H}t/\hbar} \hat{\rho} e^{i\hat{H}t/\hbar} \right] \\
&= -\frac{i\hat{H}}{\hbar} e^{-i\hat{H}t/\hbar} \hat{\rho} e^{i\hat{H}t/\hbar} + e^{-i\hat{H}t/\hbar} \left(\frac{i\hat{H}}{\hbar} \right) e^{i\hat{H}t/\hbar} \\
&= -\frac{i}{\hbar}\left[\hat{H}, \hat{\rho}(t) \right] \ .
\end{aligned} \tag{2.19}
$$

2.3 Phase-space Representation of Quantum Mechanics

It has been shown [33] that probability distributions for many quantum dynamical variables may approach a classical limit in certain conditions (usually in the limit $\hbar \to 0$). This is possible when using either a coordinate space representation or a momentum space representation. However, this does still not provide a full classical-like description of quantum mechanics. In classical mechanics, the Hamilton equations of motion dictate a correlation between the positions and momenta of a particle:

$$
\begin{aligned}
\frac{dp}{dt} &= -\frac{\partial}{\partial q} H(q, p, t) \;, \\
\frac{dq}{dt} &= \frac{\partial}{\partial p} H(q, p, t) \;.
\end{aligned}
\tag{2.20}
$$

This correlation is manifested in probability distributions of both variables, known as phase-space distributions. To obtain a complete classical description of quantum systems, it must hence be possible to describe quantum dynamics in phase-space [33]. Of the many attempts to achieve this, one of the most successful was by Eugene Wigner.

2.3.1 The Wigner Representation

In standard formulations of quantum mechanics, wave functions and probability densities are given most commonly in terms of the coordinate representation [31]:

$$
\psi(x) = \langle x | \psi \rangle, \quad P(x) = |\psi(x)|^2 \;.
\tag{2.21}
$$

If $\psi(x)$ is known, it is a simple matter of performing a Fourier transform to obtain the wave function in the momentum representation:

$$\psi(p) = \frac{1}{\sqrt{\hbar}} \int e^{-ixp/\hbar}\psi(x)dx \;, \tag{2.22}$$

and hence the momentum probability density $|\psi(p)|^2$.

It is desirable to obtain a representation where the probability density is given as a function of both these dynamical variables. This quantum phase-space probability density would have to obey the constraints that it is everywhere positive, and normalised over phase-space, for it to be interpreted as a probability distribution. In addition to this, it would have to be possible to use it to calculate expectation values, since all the information of a quantum system is given by quantum averages of physical observables.

Before the Wigner function can be introduced, the Weyl transform needs to be defined. For an arbitrary operator $\hat{\chi}$, this transform is [31]

$$\tilde{\chi}(x,p) = \int e^{-ipy/\hbar}\langle x + y/2|\hat{\chi}|x - y/2\rangle dy \;, \tag{2.23}$$

where the tilde denotes the Weyl transform. Here it is done for an operator which is represented in the position basis, although this transform can also be applied to an operator whose matrix elements are given in the momentum basis. The Weyl transform thus provides a way to convert a quantum operator to a function of phase-space. This was a historical step in the field of quantum mechanics. Prior to this representation, quantum mechanics was described only using operators acting on wave functions in coordinate space (Schrödinger), or operators given by matrices (Heisenberg). When Wigner first introduced his representation in 1932, it was the first time that it was proven that quantum mechanics could be described by functions, and not operators.

The Wigner function for a single particle is defined as the Weyl transform of the density matrix divided by Planck's constant [32]:

$$
\begin{aligned}
W(x,p) &= \frac{1}{h}\int e^{ipy/\hbar}\langle x+y/2|\hat{\rho}|x-y/2\rangle dy \\
&= \frac{1}{h}\int e^{ipz/\hbar}\langle p+z/2|\hat{\rho}|p-z/2\rangle dz \ . \quad (2.24)
\end{aligned}
$$

An important characteristic of the Weyl transform is that the integral over phase-space of the product of Weyl transforms of two operators is equivalent to the trace of the product of these two operators [31]:

$$
Tr\left(\hat{A}\hat{B}\right) = \frac{1}{h}\int\int \tilde{A}(x,p)\tilde{B}(x,p)dx\,dp \ . \quad (2.25)
$$

This identity provides a way to calculate expectation values using the Wigner function:

$$
\begin{aligned}
Tr\left(\hat{\rho}\hat{\chi}\right) &= \frac{1}{h}\int\int \tilde{\rho}(x,p)\tilde{\chi}(x,p)dx\,dp \\
&= \int\int \tilde{W}(x,p)\tilde{\chi}(x,p)dx\,dp \ , \quad (2.26)
\end{aligned}
$$

thereby fulfilling one of the conditions for a phase-space probability density.

The Wigner function is also normalised over phase-space. For it to be possible to interpret the Wigner function as a probability function, this must be so. It is a simple matter to prove this property:

If the Weyl transform of the identity matrix is taken, we find that it is equal to 1:

$$
\begin{aligned}
\tilde{1} &= \int e^{-ipy/\hbar}\langle x+y/2|\hat{1}|x-y/2\rangle \\
&= \int e^{-ipy/\hbar}\delta(y)\,dy = 1 \ . \quad (2.27)
\end{aligned}
$$

This can be used in conjunction with Eq. (2.25) to obtain

$$
Tr\left(\hat{\rho}\hat{1}\right) = \frac{1}{h}\int\int \tilde{\rho}(x,p)\tilde{1}dx\,dp
$$

$$= \int\int W(x,p)dx\,dp = 1 \;, \qquad\qquad (2.28)$$

because of Eq. (2.15). It is also possible to determine whether or not the system is in a pure state by using the Wigner function and the condition (2.16). The integral over phase-space of the square of the Wigner function can be expressed in terms of $Tr(\hat{\rho}^2)$:

$$\int\int W(x,p)^2 dx\,dp \;=\; \frac{1}{h}\left(\frac{1}{h}\int\int \tilde{\rho}(x,p)\tilde{\rho}(x,p)dx\,dp\right)$$
$$=\; \frac{1}{h}Tr\left(\hat{\rho}^2\right) = \frac{1}{h}\;, \qquad\qquad (2.29)$$

when $Tr\left(\hat{\rho}^2\right)=1$. Thus Eq. (2.29) gives the condition for a pure state.

From the above properties, it might be tempting to interpret the Wigner function as a probability density. However, it is not possible to do so, due to a particular characteristic. Consider two orthogonal states of a system ψ_1 and ψ_2. There will be a density operator associated with each state, given by $\hat{\rho}_1$ and $\hat{\rho}_2$. Using Eqs. (2.24) and (2.25) we obtain

$$Tr\left(\hat{\rho}_1\hat{\rho}_2\right) = \frac{1}{h}\int\int hW_1(x,p)hW_2(x,p)dx\,dp \;. \qquad\qquad (2.30)$$

But $Tr\left(\hat{\rho}_1\hat{\rho}_2\right) = |\langle\psi_1|\psi_2\rangle|^2$, and for orthogonal states this is equal to zero. Thus,

$$\int\int W_1(x,p)W_2(x,p)dx\,dp = 0 \;. \qquad\qquad (2.31)$$

This of course implies that $W_1(x,p)$ or $W_2(x,p)$, or both, must be negative for some regions of phase-space. Obviously this denies the interpretation of the Wigner function as a probability density. One might find this property peculiar considering that the diagonal elements of the density operator are always positive, but it must be remembered that the off-diagonal elements of the density matrix are not positive definite, and it is these elements which

cause the Wigner function to be negative in some regions of phase-space.

Because equations of motions in quantum mechanics are given in terms of products of operators, it must be possible to represent this in the Wigner representation as well. If we consider 2 operators $\hat{A}$ and $\hat{B}$, the Wigner transform of their product is [9]

$$
\begin{aligned}
(\hat{A}\hat{B})_W &= A(R,P)e^{\frac{\hbar\Lambda}{2i}}B(R,P) \\
&= B(R,P)e^{-\frac{\hbar\Lambda}{2i}}A(R,P) \,,
\end{aligned}
\tag{2.32}
$$

where the subscript W denotes the Wigner transform, and $\Lambda = -(\frac{\overleftarrow{\partial}}{\partial R}\frac{\overrightarrow{\partial}}{\partial P} - \frac{\overleftarrow{\partial}}{\partial P}\frac{\overrightarrow{\partial}}{\partial R}$ is the negative of the Poisson bracket. This identity also applies for the partial Wigner representation, which is discussed below.

2.3.2 The Partial Wigner Representation

The partial Wigner representation is very useful in quantum-classical studies [34]. It stems from the more general Wigner formulation of quantum mechanics. When considering a system where a quantum subsystem of interest is interacting with an environment, it is usually impossible to obtain a fully quantum-mechanical solution. When the particles constituting the environment are much more massive than those of the subsystem, it is much more convenient to treat the environmental degrees of freedom classically. To this end, a partial Wigner transform can be performed. This is done by taking the Weyl function over only the bath coordinates of the system. The Hamiltonian is thus converted from a full quantum-mechanical operator to an operator of the Hilbert space of the subsystem, as well as a function of phase-space variables for the bath:

$$
\hat{H}(\hat{R},\hat{P},\hat{q},\hat{p}) \to H_W(R,P,\hat{q},\hat{p}) \,,
\tag{2.33}
$$

where the subscript W denotes the partial Wigner transformed Hamiltonian. The lower case variables denotes the coordinates for the quantum subsystem, while the upper case variables denote those of the bath. As is evident in the above equation, the operators of the quantum subsystem remain unchanged, and thus the subsystem is treated quantum-mechanically, as desired.

For a subsystem comprising a quantum subsystem coupled to an environment of N particles, the partial Wigner transform for the density matrix is given by

$$\hat{\rho}_W(R, P) = (2\pi\hbar)^{-3N} \int dz \, e^{iP \cdot z/\hbar} \langle R - \frac{z}{2} | \hat{\rho} | R + \frac{z}{2} \rangle \, . \qquad (2.34)$$

Note that the change from a single particle to N particles means that all variables must be interpreted as vectors of dimension $3N$, and the factor $(2\pi\hbar)^{-1}$ becomes $(2\pi\hbar)^{-3N}$ [33].

For an operator of the system,

$$\hat{\chi}(R, P) = \int dz \, e^{iP \cdot z/\hbar} \langle R - \frac{z}{2} | \hat{\chi} | R + \frac{z}{2} \rangle \, . \qquad (2.35)$$

In this representation, $\hat{\chi}$ is both an operator on the Hilbert space of the subsystem, and an operator of phase-space. Equations (2.34) and (2.35) for the density matrix and operators are ideal for working with quantum-classical systems, due to the ability to treat the bath coordinates classically. Naturally, since the forms of the operator and density matrix have been altered, so should their respective equations of motion. Indeed, their time evolution is no longer governed by the quantum commutator, but rather by the quantum-classical bracket. It is interesting to note that this bracket is non-Hamiltonian in nature, as opposed to the commutator of quantum mechanics and analogous Poisson bracket of classical mechanics. This will be demonstrated in the following section.

2.4 Hamiltonian Theory, Non-Hamiltonian Theory and the Quantum-Classical Bracket

2.4.1 Hamiltonian Theory

The purpose of describing any system mathematically, be it in the realm of classical mechanics or quantum mechanics, is to be able to predict values for properties of that system that are measurable experimentally. In general, we consider a system subject to external influences, and wish to describe how this system evolves in time. These measurable properties are given by ensemble averages. In both quantum or classical mechanics, we use linear response theory to obtain ensemble averages in terms of time correlation functions. However, linear response theory requires that the formalism used to describe the dynamics should be invariant under time translation. A theory with this property is known as a Hamiltonian theory. Due to this constraint of linear response theory, formalisms used for quantum mechanics and classical mechanics are Hamiltonian.

Quantum mechanics and classical mechanics share an analogous algebraic bracket structure [35]; classical theory is governed by the Poisson bracket, and quantum theory by the commutator bracket. The condition for a theory to be Hamiltonian is that the algebra of its bracket must constitute a Lie algebra. Consider a mathematical space, of which the elements $\{A, B, C\}$ are a part. A Lie algebra for this space is one which possesses the following properties [36]:

$$(A, B) = -(B, A) \ , \tag{2.36}$$

$$\lambda(A, B) = (\lambda A, B) = (A, \lambda B) \ , \tag{2.37}$$

$$(A + B, C) = (A, C) + (B, C) \ . \tag{2.38}$$

Here $(.., ..)$ denotes a generic bracket, which could be classical or quantum

in nature and λ is a c-number. In addition to the above there properties, the Jacobi relation must also hold; that is,

$$\mathcal{J} = ((A,B),C) + ((C,A),B) + ((B,C),A) = 0 . \qquad (2.39)$$

An algebra may thus satisfy the first three properties given by Eqs. (2.36-2.38), but it is only a Lie algebra (and consequently a Hamiltonian theory) if the Jacobi relation is also fulfilled.

Equations (2.37) and (2.38) imply that the bracket is a linear operator of its space, and of c-numbers. The antisymmetric property (2.36) of the bracket is important for defining time evolution. When the elements of the space of the bracket are not explicitly dependent on time, then time evolution can be given choosing by an element H, and defining the equations of motion by [36]:

$$\frac{dA}{dt} = (A,H) , \qquad (2.40)$$

with H usually chosen to be the Hamiltonian.

Two elements A and B, which are in the space of the algebra defined by the bracket $(..,..)$, are constants of motion if and only if

$$\dot{A} = (A,H) = 0 \qquad \dot{B} = (B,H) = 0 , \qquad (2.41)$$

where a dot denotes a time derivative. H is generally (but not necessarily) taken to be the Hamiltonian. The requirement of time translation invariance is that this further then implies that (A,B) is also a constant of motion:

$$((A,B),H) = 0 . \qquad (2.42)$$

We can confirm directly that this condition is satisfied by any Lie algebra,

since from the Jacobi relation we have

$$
\begin{aligned}
((A,B),H) &= -((H,A),B) - ((B,H),A) \\
&= ((A,H),B) - ((B,H),A) \\
&= (\dot{A},B) - (\dot{B},A) = 0 \ . \quad (2.43)
\end{aligned}
$$

2.4.2 Non-Hamiltonian Theory

Now that the algebra for a Hamiltonian theory has been defined, it is possible to introduce non-Hamiltonian theories. Simply put, these are theories for which the Jacobi relation does not hold,

$$
\mathcal{J} = ((A,B),C) + ((C,A),B) + ((B,C),A) \neq 0 \ . \quad (2.44)
$$

It is easy to show, using Eqs. (2.41) and (2.44), that if A and B are constants of motion, then it is impossible for (A,B) to be a constant of motion. As a result, the time translation property no longer holds. We thus see that the Jacobi relation is not only an indication of time translation invariance, it is indeed a requirement of it.

It might not seem intuitive to choose to use a non-Hamiltonian theory over a Hamiltonian one, since time translation invariance is a very useful property. However, the advantages of non-Hamiltonian theories become apparent when considering simulations of systems with a large number of coordinates. When implementing thermodynamic constraints on a system, Hamiltonian theory dictates that an infinite number of degrees of freedom should be considered. Using a non-Hamiltonian formalism, on the other hand, it has been shown that the same constraints can be achieved, with only a small number of degrees of freedom [35] [37]. In quantum dynamics it is an arduous task to simulate even a small number of degrees of freedom, with larger numbers becoming impossible due to computational constraints.

It is possible to circumvent this problem by using non-Hamiltonian quantum-classical methods.

2.4.3 The Quantum-Classical Liouville Equation and the Quantum-Classical Bracket

In light of the fact that the bracket associated with a quantum-classical formalism must describe a system that is partly quantum and partly classical in nature, it would not be unreasonable to assume that its form would in some way resemble that of the classical Poisson bracket and the quantum commutator bracket. To better understand the quantum-classical bracket it is thus convenient to first consider the brackets of quantum and classical mechanics.

It has long been known that the symplectic nature of the Poisson bracket allows it to be easily cast into matrix form [38][39]. For any two functions f and g of phase-space,

$$\{f, g\} = \begin{bmatrix} \frac{\partial f}{\partial R} & \frac{\partial g}{\partial P} \end{bmatrix} \cdot \mathcal{B}^c \cdot \begin{bmatrix} \frac{\partial f}{\partial P} \\ \frac{\partial g}{\partial R} \end{bmatrix} , \qquad (2.45)$$

where $\mathcal{B}^c$ is the symplectic matrix

$$\mathcal{B}^c = \begin{bmatrix} 0 & 1 \\ -1 & 0 \end{bmatrix} . \qquad (2.46)$$

Any bracket that can be written in terms of the symplectic matrix in such a way is symplectic.

It has been shown [35] that the quantum commutator is also symplectic, and can therefore be written as

$$[A, B] = \begin{bmatrix} A & B \end{bmatrix} \cdot \mathcal{B}^c \cdot \begin{bmatrix} A \\ B \end{bmatrix} . \qquad (2.47)$$

When expressed this way, it is easy to see the similarity in the algebraic structures of quantum and classical mechanics. It is interesting to note that the symplectic form for the bracket is a requirement for the equations of motion to be canonical, but not for it be a Lie algebra. If a bracket is symplectic, however, then it constitutes a Lie algebra. This is illustrated in Fig. 2.1 below.
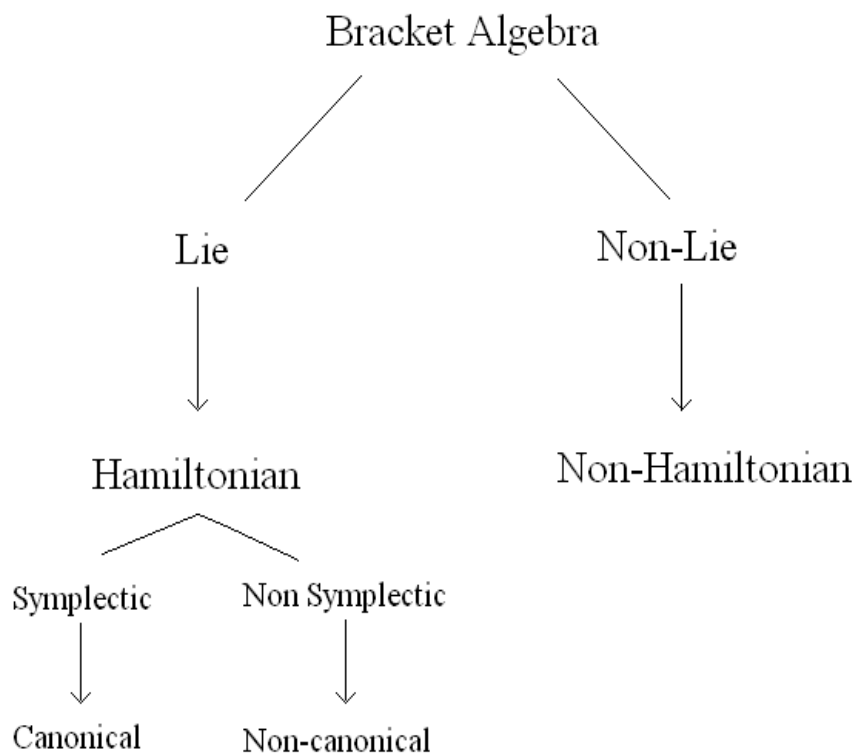

Figure 2.1: The bracket algebra may be broken up into two main groups - Lie (or Hamiltonian) algebras and non-Lie (non-Hamiltonian) algebras. Hamiltonian algebras can further be split into those that can be cast into a symplectic form, and those that cannot. Whether or not a bracket is symplectic then dictates whether its corresponding equations of motion are canonical. Note that if a bracket is symplectic, it implies that it is a Lie algebra, but the reverse is not true.

Noting that both the quantum and classical bracket can be written in

this matrix form, it is not unreasonable to assume that this can also be done for the quantum-classical bracket. With this in mind, we can define a generalised bracket [35] with the form

$$(A, B) = \begin{bmatrix} A & B \end{bmatrix} \cdot \mathcal{K} \cdot \begin{bmatrix} A \\ B \end{bmatrix} , \qquad (2.48)$$

where $\mathcal{K}$ is an antisymmetric matrix

$$\mathcal{K} = \begin{bmatrix} 0 & \hat{\zeta} \\ -\hat{\zeta} & 0 \end{bmatrix} , \qquad (2.49)$$

and then write equations of motion in terms of this bracket. Note that $\hat{\zeta}$ can be an operator or a c-number.

We wish to cast the quantum-classical bracket in this form. First, consider a system defined by the total Hamiltonian operator

$$\hat{H} = \hat{H}_S + \hat{H}_B + \hat{H}_{SB} , \qquad (2.50)$$

where the subscripts S,B and SB stand for the subsystem, bath and coupling interaction respectively. The equation of motion for the density matrix $\hat{\rho}$ is given by the von Neumann equation, which in matrix from, is

$$\frac{\partial \hat{\rho}}{\partial t} = -\frac{i}{\hbar} \begin{bmatrix} \hat{H} & \hat{\rho} \end{bmatrix} \cdot \mathcal{B}^c \cdot \begin{bmatrix} \hat{H} \\ \hat{\rho} \end{bmatrix} . \qquad (2.51)$$

We assume that the bath Hamiltonian is dependent upon a pair of canonically conjugate operators $\hat{R}, \hat{P}$, with a coupling of form $\hat{H}_{SB} = \hat{H}_{SB}(\hat{R})$. Since we wish to consider quantum-classical dynamics, it would be convenient to express the bath Hamiltonian in terms of the classical phase-space coordinates, and to this end we perform a partial Wigner transform over the bath coordinates $\hat{R}$ and $\hat{P}$. The partial Wigner transformed Hamiltonian of the system is given by

$$\hat{H}_W(X) = \hat{H}_S + H_{W,B}(X) + \hat{H}_{W,SB}(R) \ . \qquad (2.52)$$

Here, the symbol X has been used to denote the canonically conjugate classical phase-space variables (R, P). Making use of the identity in Eq. (2.32), the evolution equation for the density matrix becomes

$$\frac{\partial}{\partial t}\hat{\rho}_W(X, t) = -\frac{i}{\hbar}\left[\begin{array}{cc} \hat{H}_W(X) & \hat{\rho}_W(X, t) \end{array}\right] \cdot \mathcal{D} \cdot \left[\begin{array}{c} \hat{H}_W(X) \\ \hat{\rho}_W(X, t) \end{array}\right] ,$$
$$(2.53)$$

where

$$\mathcal{D} = \left[\begin{array}{cc} 0 & e^{\frac{i\hbar}{2}\overleftarrow{\partial}_k \mathcal{B}^c_{kj} \overrightarrow{\partial}_j} \\ -e^{\frac{i\hbar}{2}\overleftarrow{\partial}_k \mathcal{B}^c_{kj} \overrightarrow{\partial}_j} & 0 \end{array}\right] . \qquad (2.54)$$

In the above equation, the symbols $\overleftarrow{\partial}_j$ and $\overrightarrow{\partial}_j$ denote the derivative $\partial/\partial X_j$ with respect to the phase-space point coordinates, acting to left and right respectively. Here, and in the following, repeated indices imply summation.

We see that the matrix $\mathcal{D}$ is not symplectic, and hence the associated equations of motion are not canonical. However, Eq. (2.53) is still a Lie algebra, and thus it is Hamiltonian (see Fig. (2.1)).

Equation (2.53) displays a mixed Wigner-Heisenberg representation of quantum mechanics, where the operators also contain a functional dependence on the phase-space coordinates. This representation is equivalent to that of Heisenberg, but calculations are usually very difficult to perform when the equations are written this way. However, if (i) the bath Hamiltonian is quadratic

$$\hat{H}_{W,B} = \sum_{j=1}^{N} \left(\frac{P_j^2}{2} + \frac{\omega_j^2 R_j^2}{2} \right) , \tag{2.55}$$

and (ii) the interaction Hamiltonian is of the form

$$\hat{H}_{W,SB} = V_B(R) \otimes \hat{H}_S' , \tag{2.56}$$

with (iii) $V_B(R)$ being at most a quadratic function of R, and (iv) $\hat{H}_S'$ acts only in the Hilbert space of the subsystem, then an expansion of the exponential terms in the matrix $\mathcal{D}$ can be taken up to linear order. Equation (2.53) can then be rewritten as [25]

$$\frac{\partial}{\partial t}\hat{\rho}_W(X,t) = -\frac{i}{\hbar} \left[\begin{array}{cc} \hat{H}_W(X) & \hat{\rho}_W(X,t) \end{array} \right] \cdot \mathcal{D}_{lin} \cdot \left[\begin{array}{c} \hat{H}_W(X) \\ \hat{\rho}_W(X,t) \end{array} \right] , \tag{2.57}$$

with

$$\mathcal{D}_{lin} = \left[\begin{array}{cc} 0 & 1 + \frac{i\hbar}{2} \overleftarrow{\partial}_k \, \mathcal{B}_{kj}^c \, \overrightarrow{\partial}_j \\ -1 - \frac{i\hbar}{2} \overleftarrow{\partial}_k \, \mathcal{B}_{kj}^c \, \overrightarrow{\partial}_j & 0 \end{array} \right] . \tag{2.58}$$

This linear expansion is exact for Hamiltonians, satisfying conditions (i) to (iv), as the higher order terms go to zero when operated on $\hat{H}_W(X)$. The evolution equation (2.57) is the quantum-classical Liouville equation, and in general it is easier to simulate numerically than Eq. (2.53). Equation (2.57) can also be written in terms of the quantum commutator bracket, and the classical Poisson bracket:

$$\begin{aligned} \frac{\partial}{\partial t}\hat{\rho}_W(X,t) &= -\frac{i}{\hbar}[\hat{H}_W, \hat{\rho}_W] + \frac{1}{2}\left(\{\hat{H}_W, \hat{\rho}_W\} - \{\hat{\rho}_W, \hat{H}_W\}\right) \\ &= -\left(\hat{H}_W, \hat{\rho}_W\right) \\ &= -i\mathcal{L}\hat{\rho}_W(X,t) . \end{aligned} \tag{2.59}$$

In the second line above, the quantum-classical bracket has been defined as a combination of the quantum and classical brackets. The last line introduces the quantum-classical Liouville superoperator $\mathcal{L}$. Note that since $\mathcal{D}_{lin}$ is of the same form as $\mathcal{K}$ in (2.49), the quantum-classical bracket is in the class of general bracket defined by Eq. (2.48). However, the quantum-classical bracket no longer obeys the Jacobi relation (2.39) [35]; it is thus not a Lie algebra, and is therefore non-Hamiltonian. The violation of this relation is not to a great extent, however, and a more accurate term would be approximately Hamiltonian. This accounts for the fact that certain dynamical properties of systems that require linear response theory can still be computed within this formalism.

Note that the conversion of the Heisenberg equation into the partial Wigner representation is performed in exactly the same way as that of the von Neumann equation, except for a change in sign. We thus have for an arbitrary operator $\hat{\chi}$

$$\frac{\partial}{\partial t}\hat{\chi}_W(X,t) \;=\; \left(\hat{H}_W,\hat{\chi}_W\right) = i\mathcal{L}\hat{\chi}_W(X,t)\,. \tag{2.60}$$

Chapter 3

Numerical Algorithms for Nonadiabatic Dynamics

This chapter begins by discussing briefly two bases convenient for quantum-classical simulations. Emphasis will be placed on the adiabatic basis, and show how it naturally leads to the formation of surface-hopping algorithms. The evolution equation for the density matrix will be solved in such a way that the form is convenient for computational use. The momentum-jump approximation of the J-operator will then be introduced, which provides a way of implementing this operator in numerical calculations. Finally, the sequential short-time propagation algorithm will be discussed, which was used in the project work.

3.1   Representation into a Basis

If the Hamiltonian is time independent, then so is the quantum-classical Liouville superoperator $\mathcal{L}$ introduced above. Then Eqs. (2.53) and (2.60) have formal solutions

$$\hat{\rho}_W(R, P, t) \;=\; e^{-i\hat{\mathcal{L}}t}\hat{\rho}_W(R, P, 0) \;, \tag{3.1}$$

and

$$\hat{\chi}_W(R, P, t) \;=\; e^{i\hat{\mathcal{L}}t}\hat{\chi}_W(R, P, 0) \;, \tag{3.2}$$

where $\hat{\rho}_W(R, P, 0)$ and $\hat{\chi}_W(R, P, 0)$ denotes the density matrix and operator respectively, at time zero.

As it stands, these equations are abstract, and to perform numerical calculations, we need to rotate them into a basis. In terms of a set of basis vectors $|\alpha\rangle$ which span the Hilbert space of the quantum subsystem, Eqs. (3.1) and (3.2) are

$$\hat{\rho}_W^{\alpha\alpha'}(R, P, t) \;=\; \sum_{\beta\beta'} \left(e^{-i\hat{\mathcal{L}}t}\right)_{\alpha\alpha',\beta\beta'} \hat{\rho}_W^{\beta\beta'}(R, P, 0) \;, \tag{3.3}$$

and

$$\hat{\chi}_W^{\alpha\alpha'}(R, P, t) \;=\; \sum_{\beta\beta'} \left(e^{i\hat{\mathcal{L}}t}\right)_{\alpha\alpha',\beta\beta'} \hat{\chi}_W^{\beta\beta'}(R, P, 0) \;. \tag{3.4}$$

Of course, the choice of basis used in numerically simulating the dynamics of a given system is governed by the type of problem being investigated. Two bases that are very convenient for simulations of quantum-classical dynamics are the subsystem basis and the adiabatic basis.

3.1.1 The Subsystem Basis

As the name indicates, the subsystem basis is given by the solutions of the eigen value equation for the subsystem Hamiltonian:

$$\hat{H}_S|\alpha\rangle = \epsilon_\alpha|\alpha\rangle . \tag{3.5}$$

In this basis, the quantum-classical Liouville superoperator is given by [34]

$$
\begin{aligned}
-i\mathcal{L}_{\alpha\alpha',\beta\beta'} &= -\left(i\tilde{\omega}_{\alpha\alpha'} + iL_b\right)\delta_{\alpha\beta}\delta_{\alpha'\beta'} + \delta_{\alpha\beta}\left(\frac{i}{\hbar}V_c^{\beta'\alpha'} + \frac{1}{2}\frac{\partial V_c^{\beta'\alpha'}}{\partial R}\cdot\frac{\partial}{\partial P}\right) \\
&+ \delta_{\alpha'\beta'}\left(-\frac{i}{\hbar}V_c^{\alpha\beta} + \frac{1}{2}\frac{\partial V_c^{\alpha\beta}}{\partial R}\cdot\frac{\partial}{\partial P}\right) .
\end{aligned}
\tag{3.6}
$$

Here $\tilde{\omega}_{\alpha\alpha'} = (\epsilon_\alpha - \epsilon_{\alpha'})/\hbar$, $V_c^{\alpha\beta} = \langle\alpha|\hat{V}_c|\beta\rangle$, and L_b is a Liouville operator responsible for the classical evolution of the bath:

$$iL_b = \frac{P}{M}\frac{\partial}{\partial R} - \frac{\partial V_b}{\partial R}\frac{\partial}{\partial P} , \tag{3.7}$$

where V_b is the potential energy of the bath. For a system with a large number of classical bath coordinates, this is not the most convenient basis to use. However, this is a useful basis when considering a quantum subsystem coupled to a single environmental coordinate, such as an electromagnetic mode or a thermostat.

3.1.2 The Adiabatic Basis

When considering dynamics of a system in which the bath comprises many classical coordinates, it is convenient to utilise the adiabatic basis. It shall be seen that this basis leads naturally to the formulation of so-called surface-hopping schemes, a common type of algorithm used in simulating quantum-classical dynamics. The adiabatic Hamiltonian $\hat{h}_W$ is given by

$$\hat{h}_W(R) = \hat{h}_s + V_b(R) + \hat{V}_c(R) , \tag{3.8}$$

and the adiabatic basis is defined by the eigenvalue equation

$$\hat{h}_W(R)|\alpha; R\rangle = E_\alpha(R)|\alpha; R\rangle \ . \tag{3.9}$$

In this basis, the quantum-classical Liouville superoperator is given by [34]

$$
\begin{aligned}
-i\mathcal{L}_{\alpha\alpha',\beta\beta'} &= -(i\omega_{\alpha\alpha'} + iL_{\alpha\alpha'})\delta_{\alpha\beta}\delta_{\alpha'\beta'} + J_{\alpha\alpha',\beta,\beta'} \\
&= -i\mathcal{L}^0_{\alpha\alpha'}\delta_{\alpha\beta}\delta_{\alpha'\beta'} + J_{\alpha\alpha',\beta\beta'} \ .
\end{aligned}
\tag{3.10}
$$

In the last line, the adiabatic quantum classical Liouville superoperator $\mathcal{L}^0$ has been introduced: it describes purely adiabatic dynamics. The derivation of Eq. (3.10) can be found in Appendix B.

The quantum-classical Liouville superoperator (3.10) contains three terms. Firstly, the Bohr frequency, obtained from the difference in energies of the adiabatic states -

$$\omega_{\alpha\alpha'}(R) = \frac{E_\alpha(R) - E_{\alpha'}(R)}{\hbar} \ . \tag{3.11}$$

This term will give rise to a phase factor multiplying the operator being acted upon, when $\alpha \neq \alpha'$. The second term is the classical-like Liouville operator

$$iL_{\alpha\alpha'} = \frac{P}{M} \cdot \frac{\partial}{\partial R} + \frac{1}{2}\left(F_W^\alpha + F_W^{\alpha'}\right) \cdot \frac{\partial}{\partial P} \ , \tag{3.12}$$

which realises the evolution of the bath determined by the average of the Hellmann-Feynman forces for states α and α'. The final term is the operator responsible for nonadiabatic transitions between the energy levels of the quantum subsystem as a result of coupling to the bath. It is given by

$$
\begin{aligned}
J_{\alpha\alpha',\beta\beta'} = &- \frac{P}{M} \cdot d_{\alpha\beta}(R)\left(1 + \frac{1}{2}\frac{\Delta E_{\alpha\beta}(R)\hat{d}_{\alpha\beta}(R)}{\frac{P}{M} \cdot \hat{d}_{\alpha\beta}(R)} \cdot \frac{\partial}{\partial P}\right)\delta_{\alpha'\beta'} \\
&- \frac{P}{M} \cdot d^*_{\alpha'\beta'}(R)\left(1 + \frac{1}{2}\frac{\Delta E_{\alpha'\beta'}(R)\hat{d}^*_{\alpha'\beta'}(R)}{\frac{P}{M} \cdot \hat{d}^*_{\alpha'\beta'}(R)} \cdot \frac{\partial}{\partial P}\right)\delta_{\alpha\beta} \ .
\end{aligned}
$$

$$(3.13)$$

Here $\Delta E_{\alpha\beta}(R) = E_\alpha(R) - E_\beta(R)$, $d_{\alpha\beta}$ is the nonadiabatic coupling vector

$$d_{\alpha\beta} = \langle \alpha; R | \frac{\partial}{\partial R} | \beta; R \rangle \, , \qquad (3.14)$$

and $\hat{d}_{\alpha\beta}$ denotes its normalised form. The transition operator will be dealt with in more detail in the next section. Note that while both the adiabatic basis states and energies depend on the bath position coordinate R, this dependence will henceforth not be written explicitly, and is to be assumed.

3.2 Surface-hopping Schemes

There a number of different methods for simulating quantum-classical dynamics, such as path-integral formulations and mean-field approximations. The studies presented here focus on surface-hopping algorithms. Surface-hopping schemes are a way of solving quantum-classical dynamics in terms of trajectories in which classical evolution on single adiabatic potential energy surfaces is interspersed with nonadiabatic transitions. The evolution equation thus needs to be cast in a form convenient for this type of algorithm.

3.2.1 Solution of the Evolution Equation

As it stands, the evolution equation is

$$\rho_W(R, P, t) = e^{(-i\omega_{\alpha\alpha'} - iL_{\alpha\alpha'})\delta_{\alpha\beta}\delta_{\alpha'\beta'} + J_{\alpha\alpha',\beta\beta'}} \rho_W(R, P, t) \, , \qquad (3.15)$$

which is not a useful form for numerical calculations. The Dyson expansion can be used to obtain a more convenient form. This expansion is given by

$$e^{(\hat{A}+\hat{B})t} = e^{\hat{A}t} + \int_0^t dt' e^{\hat{A}(t-t')} \hat{B} e^{(\hat{A}+\hat{B})t'} . \tag{3.16}$$

Applying this to $e^{-i\mathcal{L}t}$ yields

$$
\begin{aligned}
(e^{-i\mathcal{L}t})_{\alpha\alpha',\beta\beta'} &= e^{-i\mathcal{L}^0_{\alpha\alpha'}t} \delta_{\alpha\beta} \delta_{\alpha'\beta'} \\
&+ \sum_{\nu\nu'} \int_0^t dt' e^{-i\mathcal{L}^0_{\alpha\alpha'}(t-t')} J_{\alpha\alpha',\nu\nu'} \left(e^{-i\mathcal{L}t'} \right)_{\nu\nu',\beta\beta'} , \tag{3.17}
\end{aligned}
$$

where

$$\mathcal{L}^0_{\alpha\alpha'} = \omega_{\alpha\alpha'} + L_{\alpha\alpha'} . \tag{3.18}$$

This Dyson integral form for the evolution operator can be incorporated into the evolution equation (3.15), which can then be solved in a perturbative way. Thus, the solution for the density matrix at time t becomes

$$
\begin{aligned}
\rho_W^{\alpha_0\alpha'_0}(R,P,t) &= e^{-i\mathcal{L}^0_{\alpha_0\alpha'_0}t} \rho_W^{\alpha_0\alpha'_0}(R,P) + \sum_{n=1}^{\infty} \\
&\times \sum_{(\alpha_1\alpha'_1)...(\alpha_n\alpha'_n)} \int_0^{t_0} dt_1 \int_0^{t_1} dt_2 ... \int_0^{t_{n-1}} dt_n \\
&\times \prod_{k=1}^{n} \left[e^{-i\mathcal{L}^0_{\alpha_{k-1}\alpha'_{k-1}}(t_{(k-1)}-t_k)} J_{\alpha_{k-1}\alpha'_{k-1},\alpha_k\alpha'_k} \right] \\
&\times e^{-i\mathcal{L}^0_{\alpha_n\alpha'_n}t_n} \rho_W^{\alpha_n\alpha'_n}(R,P) , \tag{3.19}
\end{aligned}
$$

where $\rho_W^{\alpha\alpha'}(R,P)$ is the density matrix element at time $t=0$. For an operator, the solution can be obtained in the same way except for a difference in sign which arises from the difference in sign between the Heisenberg equation (2.2) and the von Neumann equation (2.19). For an arbitrary operator $\hat{\chi}$, we thus have

$$
\begin{aligned}
\chi_W^{\alpha_0 \alpha_0'}(R,P,t) &= e^{i\mathcal{L}^0_{\alpha_0 \alpha_0'} t} \chi_W^{\alpha_0 \alpha_0'}(R,P,0) + \sum_{n=1}^{\infty} (-1)^n \\
&\times \sum_{(\alpha_1 \alpha_1')\dots(\alpha_n \alpha_n')} \int_0^{t_0} dt_1 \int_0^{t_1} dt_2 \dots \int_0^{t_{n-1}} dt_n \\
&\times \prod_{k=1}^{n} \left[e^{i\mathcal{L}^0_{\alpha_{k-1} \alpha_{k-1}'} (t_{(k-1)} - t_k)} J_{\alpha_{k-1}\alpha_{k-1}', \alpha_k \alpha_k'} \right] \\
&\times e^{i\mathcal{L}^0_{\alpha_n \alpha_n'} t_n} \chi_W^{\alpha_n \alpha_n'}(R,P,0) \,.
\end{aligned}
\tag{3.20}
$$

This iterated form of the evolution equation is more convenient for implementing in numerical simulations.

3.2.2 The SSTP Algorithm

The surface-hopping scheme studied and used to simulate the dynamics is known as sequential short-time propagation (SSTP)[27]. In this scheme, the evolution operator is broken up into a sequence of short-time propagators. The result for the entire simulation can then be obtained by concatenating these propagators.

If the time interval of study is divided into N segments each of length Δt, the evolution operator can be rewritten as [34]

$$
\left(e^{-i\mathcal{L}t} \right)_{\alpha_0 \alpha_0', \alpha_N \alpha_N'} = \sum_{(\alpha_1 \alpha_1')\cdots(\alpha_N \alpha_N')} \prod_{j=1}^{N} \left(e^{-i\mathcal{L}\Delta t} \right)_{\alpha_{j-1} \alpha_{j-1}', \alpha_j \alpha_j'} \,.
\tag{3.21}
$$

The evolution operator can be written in this way because the quantum-classical Liouville superoperator is independent of time. If Eq. (3.17) is written for a time step Δt, propagating from time $t = t_{j-1}$ to $t = t_j$ we obtain

$$
\begin{aligned}
e^{-i\mathcal{L}(t_j - t_{j-1})} &= e^{-i\mathcal{L}^0(t_j - t_{j-1})} \\
&+ \int_{t_{j-1}}^{t_j} dt' e^{-i\mathcal{L}^0(t_j - t_{j-1} - t')} J e^{-i\mathcal{L}t'} .
\end{aligned} \tag{3.22}
$$

The subscripts denoting the states have been dropped momentarily to simplify the notation. If a sufficiently small time segment is chosen, a one-point approximation can be made to the time integral above, and the Dyson series can be truncated at first order [27]. Letting $t' = t_j$, we have

$$
\begin{aligned}
e^{-i\mathcal{L}\Delta t} &= e^{-i\mathcal{L}^0 \Delta t} \\
&+ \int_{t_{j-1}}^{t_j} dt' e^{-i\mathcal{L}^0(-t_{j-1})} J e^{-i\mathcal{L}^0 t_j} .
\end{aligned} \tag{3.23}
$$

Since a one-point approximation is being made, the integrand in Eq. (3.23) can be regarded as constant, and taken out the integral. In addition to this, the order of operators can be changed. This is due to the fact that the term arising from non-commutability of the operators is higher than first order, and can therfore be disregarded. Thus

$$
\begin{aligned}
e^{-i\mathcal{L}\Delta t} &= e^{-i\mathcal{L}^0 \Delta t} + e^{-i\mathcal{L}^0 t_j} e^{-i\mathcal{L}^0(-t_{j-1})} J \int_{t_{j-1}}^{t_j} dt' \\
&= e^{-i\mathcal{L}^0 \Delta t} \left(1 + \Delta t\, J\right) .
\end{aligned} \tag{3.24}
$$

Now bringing back the subscripts for the adiabatic states, we have

$$
\left(e^{-i\mathcal{L}\Delta t}\right)_{\alpha_{j-1}\alpha'_{j-1},\alpha_j\alpha'_j} \approx e^{-i\mathcal{L}^0_{\alpha_{j-1}\alpha'_{j-1}}\Delta t} \left(\delta_{\alpha_{j-1}\alpha_j}\delta_{\alpha'_{j-1}\alpha'_j} + \Delta t J_{\alpha_{j-1}\alpha'_{j-1},\alpha_j\alpha'_j}\right) . \tag{3.25}
$$

We see that the short-time propagator is split into two terms. The first term describes completely adiabatic dynamics, while the second term realises the nonadiabaticity of the dynamics. In the adiabatic approximation $J \to 0$,

and we recover adiabatic dynamics.

Now consider the calculation of observables of the system. These are given by

$$\langle \chi \rangle(t) = \sum_{\alpha_0 \alpha_0'} \int dR\, dP\, A_W^{\alpha_0 \alpha_0'}(R, P) \rho_W^{\alpha_0 \alpha_0'}(R, P, t) \,. \qquad (3.26)$$

If the time dependence is written explicitly, and cyclic invariance of the trace is exploited, then

$$
\begin{aligned}
\langle \chi \rangle(t) &= \sum_{\alpha_0 \alpha_0'} \int dRdP\, A_W^{\alpha_0 \alpha_0'}(R, P) e^{-iHt/\hbar} \rho_W^{\alpha_0 \alpha_0'}(R, P, 0) e^{iHt/\hbar} \\
&= \sum_{\alpha_0 \alpha_0'} \int dRdP\, e^{iHt/\hbar} A_W^{\alpha_0 \alpha_0'}(R, P) e^{-iHt/\hbar} \rho_W^{\alpha_0 \alpha_0'}(R, P, 0) \\
&= \sum_{\alpha_0 \alpha_0'} \int dRdP\, A_W^{\alpha_0 \alpha_0'}(R, P, t) \rho_W^{\alpha_0 \alpha_0'}(R, P) \,. \qquad (3.27)
\end{aligned}
$$

Evidently, the difference between Eqs. (3.26) and (3.27) is that in the former the density matrix is propagated in time, with the operator remaining constant, while in the latter the reverse is true. Equation (3.27) is, in fact, a more convenient form for computational studies [34], since the initial density matrix can be used as a weight to sample phase-space points in calculating the average.

For the SSTP algorithm, the quantity $\chi_W^{\alpha_0 \alpha_0'}(R, P, t)$ is given by the discretised form of Eq. (3.20) [34], namely

$$
\begin{aligned}
\chi_W^{\alpha_0 \alpha_0'}(R, P, t) &= e^{i\mathcal{L}_{\alpha_0 \alpha_0'}^0 t} \chi_W^{\alpha_0 \alpha_0'}(R, P, 0) + \sum_{n=1}^{N} (-1)^n \sum_{(\alpha_1 \alpha_1') \cdots (\alpha_{n-1} \alpha_{n-1}')} \\
&\times \sum_{k_1=1}^{N-n+1} \sum_{k_2=k_1+1}^{N-n+2} \cdots \sum_{k_n=k_{n-1}+1}^{N} e^{i\mathcal{L}_{\alpha_0 \alpha_0'}^0 (t_{k_1}-t_0)} \left(\Delta t J_{\alpha_0 \alpha_0', \alpha_1 \alpha_1'} \right) \\
&\times e^{i\mathcal{L}_{\alpha_1 \alpha_1'}^0 (t_{k_2}-t_{k_1})} \left(\Delta t J_{\alpha_1 \alpha_1', \alpha_2 \alpha_2'} \right) \cdots \left(\Delta t J_{\alpha_{n-1} \alpha_{n-1}', \alpha_N \alpha_N'} \right) \\
&\times e^{i\mathcal{L}_{\alpha_N \alpha_N'}^0 (t-t_{k_n})} \,. \qquad (3.28)
\end{aligned}
$$

To implement this equation numerically, the J-operator needs to be considered. As it stands, it is difficult to calculate the effect of this operator in computational algorithms, and one of the solutions to this is to use the momentum-jump approximation.

3.2.3   Momentum-Jump Approximation

As stated before, the J-operator is responsible for the nonadiabatic transitions in the subsystem, and accompanying changes in the bath momentum. Inclusion of the effects of this operator in the dynamics of the system remains one of the biggest challenges to devising surface-hopping algorithms. The problem lies in the quantum back reaction; that is the way in which the bath momentum changes when a nonadiabatic transition occurs. Looking at Eq. (3.13), it can be seen that the J-operator involves bath momentum derivatives.

Intuitively, one might think of performing these derivatives using a finite difference method, so that

$$d_{\alpha\beta} \cdot \nabla_P f(P) \approx (\Delta_P)^{-1} \left[f(P + d_{\alpha\beta}\Delta_P) - f(P) \right] \ . \qquad (3.29)$$

However, this causes the trajectory to branch each time a quantum transition occurs. The method is thus highly computationally expensive for longer time calculations with the ensuing larger number of nonadiabatic transitions [1]

A more pragmatic approach involves making a so-called momentum-jump approximation, as this circumvents the branching of trajectories problem. This approximation involves changing J into an operator that shifts the bath momentum when a quantum transition occurs. To perform this conversion we consider the first term of the J-operator:

---

[1] The number of trajectories goes as 2^n, where n is the number of nonadiabatic transitions.

$$J^{1^{st}term} = \frac{P}{M} \cdot d_{\alpha\beta} \left(1 + \frac{1}{2} \frac{\Delta E_{\alpha\beta}(R)\hat{d}_{\alpha\beta}}{\frac{P}{M} \cdot \hat{d}_{\alpha\beta}} \cdot \frac{\partial}{\partial P} \right) \delta_{\alpha'\beta'} \ . \tag{3.30}$$

There are two ways to convert this operator; however, one is approximate, and does not conserve the energy of the system, while the other is exact, and does conserve the energy. Both are presented below.

Non-Conserving Momentum-Jump Approximation

In both cases, the approximation in the momentum-jump scheme is introduced by rewriting the term in brackets above as an exponential -

$$\left(1 + \frac{1}{2} \frac{\Delta E_{\alpha\beta}\hat{d}_{\alpha\beta}}{\frac{P}{M} \cdot \hat{d}_{\alpha\beta}} \cdot \frac{\partial}{\partial P} \right) \approx e^{\frac{1}{2} \frac{\Delta E_{\alpha\beta}\hat{d}_{\alpha\beta}}{\frac{P}{M} \cdot \hat{d}_{\alpha\beta}} \cdot \frac{\partial}{\partial P}} \ . \tag{3.31}$$

In the energy non-conserving rule, a further approximation is made. Since the changes in bath momentum accompanying a transition are relatively small compared to the total momentum, the term $\frac{1}{2} \frac{\Delta E_{\alpha\beta}\hat{d}_{\alpha\beta}}{\frac{P}{M} \cdot \hat{d}_{\alpha\beta}}$ is taken as a constant, and the identity

$$e^{c\frac{\partial}{\partial x}} g(x) = g(x + c) \ , \tag{3.32}$$

can be used to give

$$e^{\frac{1}{2} \frac{\Delta E_{\alpha\beta}\hat{d}_{\alpha\beta}}{\frac{P}{M} \cdot \hat{d}_{\alpha\beta}} \cdot \frac{\partial}{\partial P}} f(P) \approx f\left(P + \frac{1}{2} \frac{\Delta E_{\alpha\beta}\hat{d}_{\alpha\beta}}{\frac{P}{M} \cdot \hat{d}_{\alpha\beta}} \right) \ . \tag{3.33}$$

The J-operator is now a momentum translation operator, shifting the momentum of the jth oscillator by an amount

$$\Delta^{AMJ} P_j = \frac{1}{2} \frac{\Delta E_{\alpha\beta}\hat{d}_{\alpha\beta}^j}{\frac{P^j}{M} \cdot \hat{d}_{\alpha\beta}^j} \ . \tag{3.34}$$

Since the factor multiplying the momentum derivative on the left hand

side of (3.33) depends on P, it is not constant, and the use of identity (3.32) is an approximation, causing this momentum shift rule to violate energy conservation. The AMJ superscript denotes this approximate (and thus energy non-conserving) momentum-jump rule.

Energy-Conserving Momentum-Jump Approximation

As before, the J-operator is approximated by an exponential (see Eq. (3.31)). However, this time, the chain rule is used to express the argument of the exponential as

$$\frac{\Delta E_{\alpha\beta}\hat{d}_{\alpha\beta}}{2\frac{P}{M}\cdot\hat{d}_{\alpha\beta}}\cdot\frac{\partial}{\partial P}=\Delta E_{\alpha\beta}M\frac{\partial}{\partial(P\cdot\hat{d}_{\alpha\beta})^2}\;. \tag{3.35}$$

Here, a change of variable has been performed, and the prefactor of the differential operator in the exponential no longer depends on the bath momentum.

The J-operator is again an exponential translation operator, shifting the variable $(P\cdot\hat{d}_{\alpha\beta})^2$ by an amount $\Delta E_{\alpha\beta}M$. Therefore, the function of momentum upon which this translation operator acts needs to be rewritten as a function of $(P\cdot\hat{d}_{\alpha\beta})^2$. If the momentum vector is resolved into components parallel and perpendicular to the nonadiabatic coupling vector, we see that the J-operator has the following effect on a function of the bath momentum:

$$e^{\Delta E_{\alpha\beta}M\partial/\partial(P\cdot\hat{d}_{\alpha\beta})^2}f(P)=$$
$$f\left[P-\hat{d}_{\alpha\beta}(P\cdot\hat{d}_{\alpha\beta})+\hat{d}_{\alpha\beta}sgn(P\cdot\hat{d}_{\alpha\beta})\sqrt{(P\cdot\hat{d}_{\alpha\beta})^2+\Delta E_{\alpha\beta}M}\right]\;. \tag{3.36}$$

This gives the formula for the change in momentum associated with a quantum transition:

$$\Delta^{EMJ} P_j = -\hat{d}_{\alpha\beta}(P \cdot \hat{d}_{\alpha\beta}) + \hat{d}_{\alpha\beta} sgn(P \cdot \hat{d}_{\alpha\beta}) \sqrt{(P \cdot \hat{d}_{\alpha\beta})^2 + \Delta E_{\alpha\beta} M} \ . \quad (3.37)$$

Here the superscript EMJ denotes the exact momentum-jump rule that conserves energy in each quantum transition. For a full derivation of this rule, and a proof of energy conservation, see Appendix A.

3.2.4 Sampling Nonadiabatic Transitions

In the SSTP algorithm, the system is propagated adiabatically and at each time step a quantum transition may or may not occur. This is performed by letting the J-operator act in a stochastic way. At the end of each time step, the probability $\mathcal{P}$ is calculated to determine if a nonadiabatic transition is accepted. Naturally, this means that $\mathcal{Q} = 1 - \mathcal{P}$ gives the probability that a transition will be rejected. A primitive choice for the transition probability is

$$\mathcal{P}_{\alpha\beta}(X, \Delta t) = \frac{\left| \frac{P}{M} \cdot d_{\alpha\beta}(R) \right| \Delta t}{1 + \left| \frac{P}{M} \cdot d_{\alpha\beta}(R) \right| \Delta t} \ , \quad (3.38)$$

and correspondingly, the probability that a transition will not occur is given by

$$\begin{aligned} \mathcal{Q}_{\alpha\beta}(X, \Delta t) &= 1 - \mathcal{P}_{\alpha\beta} \\ &= \frac{1}{1 + \left| \frac{P}{M} \cdot d_{\alpha\beta}(R) \right| \Delta t} \ . \end{aligned} \quad (3.39)$$

The term $\frac{P}{M} \cdot d$ in is a measure of coupling between the bath and the subsystem. If the bath momentum lies along the nonadiabatic coupling vector, then the coupling is at a maximum and a transition is more likely. This is reflected in the transition probability $\mathcal{P}$ in Eq. (3.38), which increases monotonically with $\frac{P}{M} \cdot d$.

From (3.13), it is seen that the J-operator comprises two terms, and whenever the J-operator acts, both terms should be considered. However, this leads to a branching of trajectories. The number of trajectories that need to be considered increases as 2^n, where n is the number of times the J-operator has acted. Naturally, this is computationally undesirable, since dynamics can only be simulated for short times before running out of computer memory. A solution to this problem is to make the approximation of only acting one term of the J-operator when a transition is accepted. A natural choice is to use a probability of 1/2 for each term, to determine which term acts. For a state $(\alpha\alpha')$, the first term will change the α index to any of the other states in the Hilbert space of the system, while the second term will change the α' index. For a system with more than two states, weights are associated with each state, giving the probability of each transition the system may undergo. In the case of a two-level quantum subsystem, however, this weight is unity, since there is only one other possible state to which a transition may occur.

Chapter 4

Numerical Studies

Here will be discussed the model used to represent a particular quantum-classical system, namely the spin-boson model. The choice of system parameters is given, as well as a description of the dimensionless units used for convenience in the calculations. The observable σ_z will be introduced, for which expectation values were calculated. The results for the simulations performed using the improved sampling scheme are displayed, showing the reduced statistical error. Finally, a study of three different momentum shift rules is presented, to determine what aspects of a rule are important to obtain accurate results.

4.1 The Numerical Example

4.1.1 The Spin-Boson Model

The theory discussed thus far can be applied to any system comprising a quantum subsystem coupled to a classical environment. However, to perform numerical calculations, a model must be chosen with which the theory can be applied. The choice of model will vary, according to what is being investigated. A convenient model to use for studying general nonadiabatic quantum-classical dynamics is the spin-boson system. It is a well-studied

system [40] and thus provides a way to check the efficacy and accuracy of a simulation scheme. The spin-boson system comprises a simple two-level quantum subsystem coupled to a bath of harmonic oscillators. The subsystem is interpreted as a spin with states $\{|\uparrow\rangle, |\downarrow\rangle\}$, and the oscillators are bosons. The Hamiltonian for such a system is

$$\hat{H} = -\hbar\Omega\hat{\sigma}_x + \sum_{j=1}^{N}\left(\frac{\hat{P}_j^2}{2M_j} + \frac{1}{2}M_j\omega_j^2\hat{R}_j^2 - c_j\hat{R}_j\hat{\sigma}_z\right) , \qquad (4.1)$$

where $\hat{\sigma}_x$ and $\hat{\sigma}_z$ are the usual Pauli matrices, and Ω is a constant. The summation is over all the bath oscillators, with M_j and ω_j denoting the mass and angular frequency, respectively, of the the jth oscillator. c_j is the coupling constant giving the coupling strength between the quantum subsystem and the jth oscillator. The energy gap of the two level system is given by $2\hbar\Omega$.

The partial Wigner transformed Hamiltonian

$$\hat{H} = -\hbar\Omega\hat{\sigma}_x + \sum_{j=1}^{N}\left(\frac{P_j^2}{2M_j} + \frac{1}{2}M_j\omega_j^2 R_j^2 - c_j R_j\hat{\sigma}_z\right) , \qquad (4.2)$$

depends both on phase-space coordinates, and quantum spin degrees of freedom. This Hamiltonian can be split up into the subsystem Hamiltonian

$$\hat{h}_s = -\hbar\Omega\hat{\sigma}_x , \qquad (4.3)$$

bath Hamiltonian

$$H_b(R,P) = \sum_{j=1}^{N}\left(\frac{P_j^2}{2M_j} + \frac{1}{2}M_j\omega_j^2 R_j^2\right) , \qquad (4.4)$$

and the coupling potential

$$\begin{aligned} \hat{V}_c(R) &= -\sum_{j=1}^{N} c_j R_j\hat{\sigma}_z \\ &= \gamma(R)\hat{\sigma}_z . \end{aligned} \qquad (4.5)$$

Note that while it is possible to work with different masses for each bath coordinate, for convenience, all masses are now assumed to be the same. Thus the j subscript on the mass will henceforth be dropped.

For consistency with past work concerning dynamics of the spin-boson model, the forms of the coupling constants and frequencies of the bath oscillators were chosen to be those first used by Makri and Thompson [41]. That is,

$$\omega_j = -\omega_c \ln \left(1 - j \frac{\omega_0}{\omega_c} \right) \ , \tag{4.6}$$

and

$$c_j = \omega_j \sqrt{\xi \hbar \omega_0 M} \ , \tag{4.7}$$

with

$$\omega_0 = \frac{\omega_c}{N} \left(1 - e^{-\omega_{max}/\omega_c} \right) \ . \tag{4.8}$$

Here, ω_c is a cutoff frequency. The parameter ξ in Eq. (4.7) is a measure of strength of coupling between the quantum subsystem and the bath. It is usually known as the Kondo parameter. Equations (4.6) and (4.7) provide a way of representing a finite number of oscillators as an infinite bath of ohmic spectral density.

4.1.2 Scaled Units

Scaled (or dimensionless) un1its were used for convenience as well as accuracy. Scaled units of energy, length and time are much more appropriate for calculations for a quantum-sized system (see below), as it avoids very small numbers which then result in round-off error.

They are defined by scaling the phase-space variables (R, P) according to

$$R'_j = \left(\frac{M\omega_c}{\hbar}\right)^{\frac{1}{2}} R_j, \quad P'_j = (\hbar M\omega_c)^{-\frac{1}{2}} P_j \ . \tag{4.9}$$

This use of scaling is widespread practice in numerical simulations. In this system of units, the spin-boson Hamiltonian is given by

$$\hat{H}'_W = -\Omega'\hat{\sigma}_x + \sum_j \left(\frac{P'^2_j}{2} + \frac{1}{2}\omega'^2_j R'^2_j - c'_j\hat{\sigma}_z R'_j\right) \ , \tag{4.10}$$

where

$$\Omega' = \frac{\Omega}{\omega_c}, \quad \omega'_j = \frac{\omega_j}{\omega_c}, \quad c'_j = \omega'_j\sqrt{\xi\frac{\omega_j}{\omega_c}} \ . \tag{4.11}$$

Thus, in this system of units, effectively

$$M = \hbar = 1 \ . \tag{4.12}$$

Time and inverse temperature are also scaled, according to

$$t' = t\omega_c, \quad \beta' = \frac{\omega_c}{k_B T} \ . \tag{4.13}$$

The use of this system of scaled units is not merely for the sake of simplifying the mathematics, however. The scaling of units ensures that in the computational calculations, accuracy is not lost by multiplying very large numbers with much smaller ones. This is due to the fact that all values in the calculation are of roughly the same order.

Henceforth, only scaled units will be used and, for convenience, the primes denoting scaled units will be omitted.

4.1.3 Propagation of Trajectories

An Eulerian description of the dynamics is adopted, with the phase-space points propagated in time, and the observable calculated at the new phase-space point after each time step. Since the quantum variables of the system

also depend upon the bath coordinates, the abstract space of the system is defined so that there is a Hilbert space associated with each phase-space point (see Fig. 4.1).
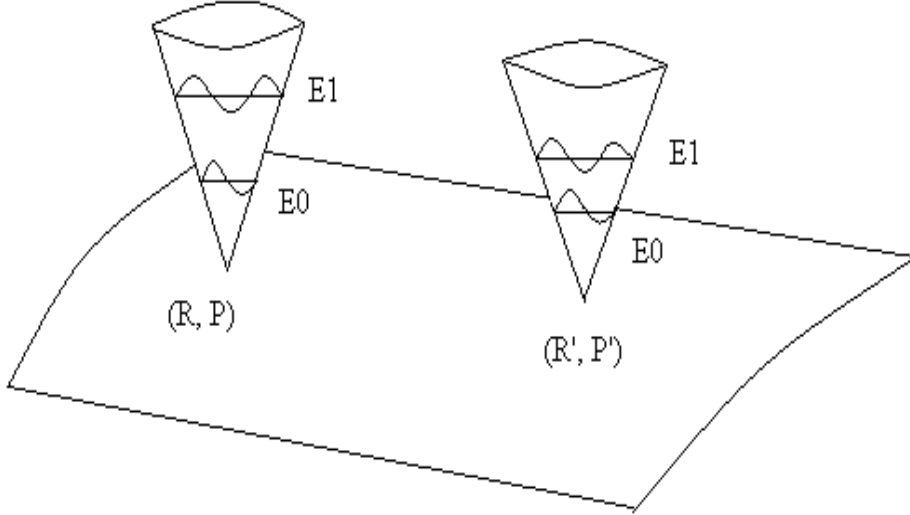

Figure 4.1: Diagrammatic representation of the abstract space for a quantum-classical spin-boson system. Due to the dependence of the quantum variables upon the bath coordinates, the quantum evolution of the Hilbert space is affected by displacements in phase-space. As an example, we see above that at a point (R, P) the energy splitting between the two energy levels is bigger than that at the point (R', P'). Evolution of the Hilbert space also affects the phase-space points via the quantum back reaction of nonadiabatic transitions.

Consider the adiabatic action of the quantum-classical Liouville super-operator for a small time Δt on an operator with a functional dependence on phase-space coordinates:

$$
\begin{aligned}
e^{i\mathcal{L}^0_{\alpha\alpha'}\Delta t}\chi_W^{\alpha\alpha'}(R,P,0) &= e^{i\omega_{\alpha\alpha'}}\chi\left(e^{iL_{\alpha\alpha'}t}R(0),e^{iL_{\alpha\alpha'}t}P(0)\right) \\
&= \mathcal{W}(t,t+\Delta t)\chi_W^{\alpha\alpha'}(R(\Delta t),P(\Delta t)) . \quad (4.14)
\end{aligned}
$$

Here, $\mathcal{W}(t, t + \Delta t)$ is a phase factor associated with the trajectory segment from t to $t + \Delta t$. If $\alpha = \alpha'$, then $\omega_{\alpha\alpha'} = 0$, and the phase factor is unity.
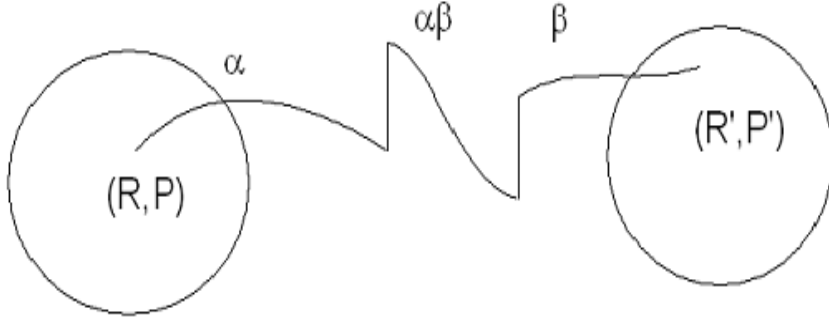

Figure 4.2: Diagrammatic representation of a single trajectory. In this example, the trajectory undergoes two nonadiabatic transitions. It begins at a phase-space point (R, P), and evolves adiabatically on an energy surface E_α. Once the first nonadiabatic transition occurs, the system evolves coherently on mean of the adiabatic energy surfaces, E_α and E_β. During this time, a phase factor $\mathcal{W}_{\alpha\beta}$ is associated with the evolution. A second nonadiabatic transition then occurs, and the system again evolves adiabatically on an energy surface E_β, ending at phase space point (R', P').

Each trajectory in the simulation begins with the bath and subsystem decoupled, with interaction beginning at $t = 0$. The initial phase-space point is obtained by sampling from the bath distribution function. The subsystem is initially in a pure state $|\uparrow\rangle$, and the bath is in thermal equilibrium. The density matrix at $t = 0$ is thus simply a product of the subsystem density matrix, and bath distribution function:

$$\hat{\rho}(0) = \hat{\rho}_s(0)\rho_b(R, P) , \qquad (4.15)$$

where

$$\hat{\rho}_s = \begin{pmatrix} 1 & 0 \\ 0 & 0 \end{pmatrix} , \qquad (4.16)$$

and the bath distribution function is given by

$$\rho_b(R, P) = \frac{e^{-\beta \hat{H}_b}}{Z_b} \ .$$

(4.17)

Here, Z_b, the bath partition function, ensures normalisation of the distribution function over phase-space. In the partial Wigner representation, the bath distribution function becomes

$$\rho_{bW}(R, P) = \prod_{j=1}^{N} \frac{\tanh\left(\beta\omega_j/2\right)}{\pi} \exp\left[-\frac{2\tanh\left(\beta\omega_j/2\right)}{\omega_j} H_b\right] \ .$$

(4.18)

The derivation for this is given in Appendix C.

The Observable $\hat{\sigma}_z$

The FORTRAN90 code written performs calculations for the observable of the operator $\hat{\sigma}_z$. Since much of the literature involving numerical simulations of the spin-boson model display results for this observable, it is easy to compare the effects of suggested improvements to the algorithm with the results already known. To understand better the physical meaning of the observable $\langle \sigma_z \rangle$, it is useful to consider an isolated two-level system. According to quantum statistical mechanics,

$$
\begin{aligned}
\langle \sigma_z \rangle &= Tr\left(\rho\chi\right) \\
&= Tr\left[\begin{pmatrix} \rho_{11} & \rho_{12} \\ \rho_{21} & \rho_{22} \end{pmatrix} \begin{pmatrix} 1 & 0 \\ 0 & -1 \end{pmatrix}\right] \\
&= Tr\begin{pmatrix} \rho_{11} & -\rho_{12} \\ \rho_{21} & -\rho_{22} \end{pmatrix} \\
&= \rho_{11} - \rho_{22} \ .
\end{aligned}
$$

(4.19)

Since the diagonal elements of the density matrix are the populations of each of the states in the system, the observable $\langle \sigma_z \rangle$ is thus the difference between the populations of the two energy levels in the system.

Rotation into the Adiabatic Basis

Since the calculations are performed in the adiabatic basis, both the operator $\hat{\sigma}_z$ and the density matrix have to be rotated into this basis. To do this, the eigenenergies and eigenvectors first need to be obtained. This is done in the usual way, by using the condition

$$\det (A - \lambda I) = 0 \qquad (4.20)$$

The adiabatic Hamiltonian for the spin-boson model is now substituted for A -

$$
\begin{aligned}
\det (A - \lambda I) &= \det \left(\hat{h}_W - \lambda I \right) \\
&= \det \left(\Omega \sigma_x + V_b(R) + \gamma(R) \hat{\sigma}_z - \lambda I \right) \\
&= \det \begin{pmatrix} V_b + \gamma(R) - \lambda & \Omega \\ \Omega & V_b - \gamma(R) - \lambda \end{pmatrix} \\
&= 0 \, .
\end{aligned} \qquad (4.21)
$$

This yields the following quadratic equation in λ,

$$
\begin{aligned}
(V_b + \gamma(R) - \lambda)(V_b - \gamma(R) - \lambda) - \Omega^2 &= 0 \\
\Rightarrow \lambda^2 - 2V_b \lambda - \gamma(R)^2 + V_b^2 - \Omega^2 &= 0 \, ,
\end{aligned} \qquad (4.22)
$$

the solutions of which are the adiabatic energies

$$\lambda = V_b \pm \sqrt{\Omega^2 + \gamma(R)^2} \, . \tag{4.23}$$

Once these energies are known, it is a simple matter of substituting them back into the eigenequation and to obtain the adiabatic basis vectors. In their normalised form, these are

$$
\begin{aligned}
|0\rangle &= \frac{1}{\sqrt{2(1+G^2)}} \begin{pmatrix} 1+G \\ 1-G \end{pmatrix} , \\
|1\rangle &= \frac{1}{\sqrt{2(1+G^2)}} \begin{pmatrix} -(1-G) \\ 1+G \end{pmatrix} .
\end{aligned} \tag{4.24}
$$

The rotation matrix $\mathbf{R}$ for the adiabatic basis is therefore

$$\mathbf{R} = \frac{1}{\sqrt{2(1+G^2)}} \begin{pmatrix} 1+G & -(1-G) \\ 1-G & 1+G \end{pmatrix} , \tag{4.25}$$

and

$$\mathbf{R}^{-1} = \frac{1}{\sqrt{2(1+G^2)}} \begin{pmatrix} 1+G & 1-G \\ -(1-G) & 1+G \end{pmatrix} . \tag{4.26}$$

The transformation of an operator into the adiabatic basis is given by

$$\hat{\chi}_{ad} = \mathbf{R}\hat{\chi}\mathbf{R}^{-1} \, . \tag{4.27}$$

By applying this transformation to the population observable and the density matrix for the subsystem we obtain

$$\sigma_z^{ad} = \frac{1}{1+G^2} \begin{pmatrix} 2G & 1-G^2 \\ 1-G^2 & 2G \end{pmatrix} , \tag{4.28}$$

and

$$\rho_s^{ad} = \frac{1}{2(1+G^2)} \begin{pmatrix} (1+G)^2 & 1-G^2 \\ 1-G^2 & (1-G)^2 \end{pmatrix} . \tag{4.29}$$

The expectation value of observable σ_z can then be evaluated using the formula

$$\langle \sigma_z^{ad}(t) \rangle = \frac{\int dRdP \rho_0(R,P) \left[\rho_0^{-1} \rho_{bW}(R,P) Tr \left(\rho_s^{ad} \sigma_z^{ad}(t) \right) \right]}{\int dRdP \rho_{bW}(R,P)} . \tag{4.30}$$

This is calculated using a Monte Carlo importance sampling scheme with importance sampling function

$$\rho_0 = \exp \left[-\beta \left(P^2/2 + E_\alpha \right) \right] . \tag{4.31}$$

4.2   Improved Sampling Scheme

As was explained in Chapter 3, the transition operator J is implemented stochastically, with a transition probability calculated at each time step of the simulation. Consider again an $\alpha \to \beta$ transition. The common choice of sampling probability used in surface-hopping schemes is given by

$$\mathcal{P}_{\alpha\beta}^0(X, \Delta t) = \frac{\left| \frac{P}{M} \cdot d_{\alpha\beta}(R) \right| \Delta t}{1 + \left| \frac{P}{M} \cdot d_{\alpha\beta}(R) \right| \Delta t} . \tag{4.32}$$

The corresponding probability that the system will not undergo a transition is

$$\begin{aligned} \mathcal{Q}_{\alpha\beta}^0(X, \Delta t) &= 1 - \mathcal{P}_{\alpha\beta}^0 \\ &= \frac{1}{1 + \left| \frac{P}{M} \cdot d_{\alpha\beta}(R) \right| \Delta t} . \end{aligned} \tag{4.33}$$

When a transition is accepted, the operator $\Delta t J$ acts, changing the quan-

tum state, and multiplying the observable by a factor of $\Delta t \frac{P}{M} \cdot d$. A factor of $\left(\mathcal{P}^0\right)^{-1}$ is then included in the observable. When a transition is rejected, however, the observable is multiplied by $\left(\mathcal{Q}^0\right)^{-1}$. While this primitive sampling scheme is sufficient for short simulation times, the concatenation of factors leads to the results becoming unstable at longer time, resulting in large statistical error. The factor $\frac{P}{M} \cdot d$ included in the observable each time a transition occurs can vary in sign and magnitude. This, combined with the oscillatory phase factor associated with each adiabatic trajectory segment, causes the main error in the results [34]. While increasing the number of trajectories in the ensemble may partially remedy this problem, it is at the cost of dramatic increases in run time. To achieve good results at longer times, the size of ensemble required becomes unrealistic.

Another partial solution is to fix a parameter n_{max}, which stipulates the number of quantum transitions a single trajectory may undergo. When a trajectory has performed n_{max} transitions, and attempts to undergo a further transition at some time $t = \tau$, its contribution to the observable is not included after this time. Again, however, this places a restriction upon the length of time that the results remain accurate. At longer times, more trajectories are truncated, and the observable is being calculated using a smaller sample size, thus increasing the statistical error.

It is possible, however, to exploit an arbitrariness in the definition of the transition probabilities (Eqs. (4.32) and (4.33)) in such a way as to filter the nonadiabatic transitions. Consider the change in energy of the system when the approximated momentum-jump rule is used for a $\alpha \to \beta$ transition:

$$\mathcal{E}_{\alpha\beta} = \sum_j \frac{(P_j + \Delta P_j)^2}{2M} + E_\alpha(R) - \left(\sum_j \frac{P^2}{2M} + E_\beta(R)\right) . \qquad (4.34)$$

New generalised transition probabilities [10] are introduced, defined as

$$\mathcal{P}_{\alpha\beta}(X, \Delta t) = \frac{\Delta t \left| \frac{P}{M} \cdot d_{\alpha\beta}(R) \right| \omega \left(c_{\mathcal{E}}, \mathcal{E}_{\alpha\beta} \right)}{1 + \Delta t \left| \frac{P}{M} \cdot d_{\alpha\beta}(R) \right| \omega \left(c_{\mathcal{E}}, \mathcal{E}_{\alpha\beta} \right)} \,, \tag{4.35}$$

and correspondingly

$$\begin{aligned} \mathcal{Q}_{\alpha\beta}(X, \Delta t) &= 1 - \mathcal{P}_{\alpha\beta} \\ &= \frac{1}{1 + \Delta t \left| \frac{P}{M} \cdot d_{\alpha\beta}(R) \right| \omega \left(c_{\mathcal{E}}, \mathcal{E}_{\alpha\beta} \right)} \,, \end{aligned} \tag{4.36}$$

where

$$\omega \left(c_{\mathcal{E}}, \mathcal{E}_{\alpha\beta} \right) = \begin{cases} 1 \text{ if } \mathcal{E}_{\alpha\beta} \leq c_{\mathcal{E}} \\ 0 \text{ otherwise} \end{cases} . \tag{4.37}$$

This amounts to disallowing any transition if $\mathcal{E}_{\alpha\beta} > c_{\mathcal{E}}$. The numerical parameter $c_{\mathcal{E}}$ thus controls the allowed amplitude for energy fluctuations accompanying a transition. To a large extent, the analytical form chosen for ω is arbitrary. In Ref. [10], the generalised sampling scheme has been based upon enforcing energy conservation upon the approximate momentum-jump rule, to within a certain numerical fluctuation. There is no set value for $c_{\mathcal{E}}$, and as such it is an adjustable constant whose value is chosen in such a way as to obtain the best results.

4.3   Study of the Improved Sampling Scheme

In this study, the SSTP algorithm was modified to include the improved nonadiabatic sampling scheme. Simulations were performed for a range of parameters, calculating the observable $\langle \sigma_z \rangle$, using both the primitive and improved sampling to demonstrate the efficacy of this scheme [25]. In the results below, the two sampling schemes are compared. In all the simulations performed, a maximum of two quantum transitions were considered for each
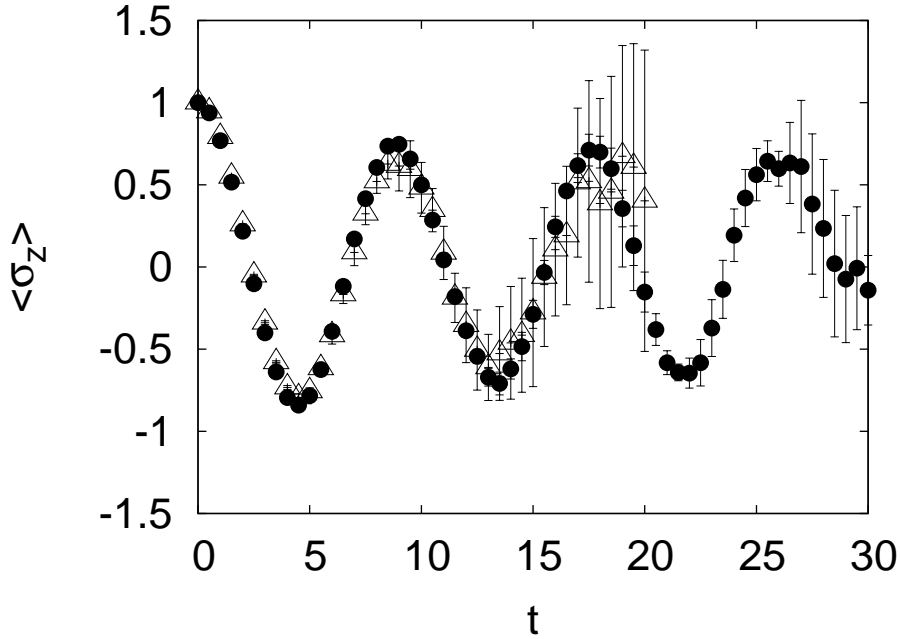
Figure 4.3: Comparison of the primitive ($\triangle$) and improved ($\bullet$) sampling schemes for the observable $\langle \sigma_z \rangle$ versus time. The vertical lines denote the standard deviation of the results. The results are for $\beta = 0.3$, $\Omega = 1/3$ and $\xi = 0.007$. A value of 0.01 for the numerical parameter $c_\mathcal{E}$ yielded the best result. Two quantum transitions were included in each trajectory. As can be seen, the error in the result for the primitive sampling grows rapidly after $t = 10$, and by $t = 20$ the result is wildly inaccurate. The statistical error for the improved sampling scheme, however, remains small up to $t = 25$, achieving reliable results for twice as long as that of the primitive sampling.

trajectory. For each set of parameters the code was run ten times, each time with a different seed for the initial conditions, so that the error in the result could be calculated. Each run comprised a phase-space ensemble of 2.5×10^4 points, and the integration time step was taken as $\Delta t = 0.01$.

Figure 4.3 displays the result of the calculations for $\beta = 0.3$, $\Omega = 1/3$ and $\xi = 0.007$. This is the same calculation as that shown in [10], and is in the realm of weak coupling between the subsystem and the bath. A value of 0.05 for the parameter $c_\mathcal{E}$ allows for reliable results to be accessed for twice as long a time period as that of the primitive sampling. This was the first
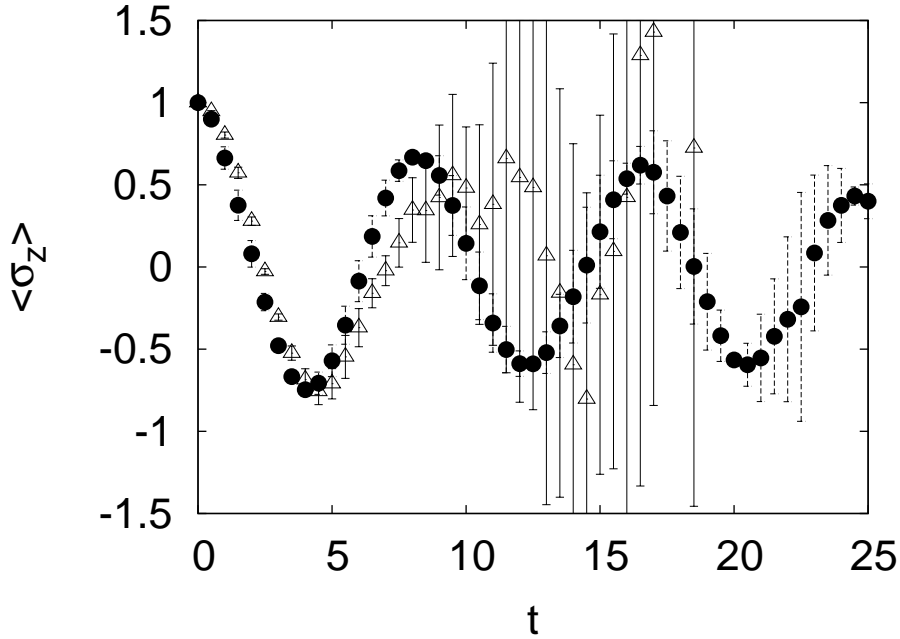
Figure 4.4: Comparison of the primitive ($\triangle$) and improved ($\bullet$) sampling schemes for the observable $\langle \sigma_z \rangle$ versus time. This plot displays the results for system parameters $\beta = 3.0$, $\Omega = 1/3$ and $\xi = 0.1$. The numerical parameter $c_{\mathcal{E}}$ was taken as 0.05. Two quantum transitions were included per trajectory. The statistical error for the primitive sampling result grows rapidly after $t = 10$ and by $t = 12$, the error is already larger than the possible range of the result, $[-1, 1]$. When the improved sampling is used, this magnitude of error is not encountered, and the result is stable for 3 times as long as that of the primitive sampling.

calculation performed. It reproduced the result from Ref. [10], showing that the improved sampling scheme had been implemented correctly.

Once this had been achieved, it was possible to run simulations for a wide ranged of parameters. In Fig. 4.4 we see the result for the population for moderate coupling. The system parameters used were $\beta = 3.0, \Omega = 1/3$ and $\xi = 0.1$. For this coupling strength, the result for the primitive sampling soon becomes unstable, and the statistical error becomes larger than the allowed ranged for the observable after $t = 12$. (Naturally, since $\langle \sigma_z \rangle$ is the fractional population difference in the two level system, it can only have a
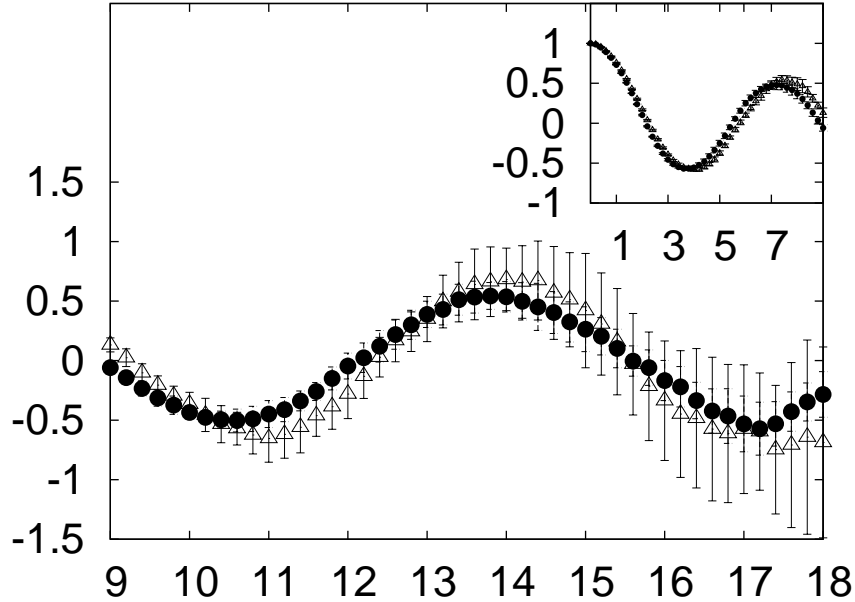
Figure 4.5: Comparison of the primitive ($\triangle$) and improved ($\bullet$) sampling schemes for the observable $\langle\sigma_z\rangle$ versus time. The calculation was performed for $\beta = 1.0$, $\Omega = 0.4$ and $\xi = 0.13$. The best result was obtained for $c_{\mathcal{E}} = 0.1$. Two quantum transitions were included per trajectory. The inset shows the results for the two sampling schemes at short time, where they both agree, with small statistical error. The main figure shows the long-time dynamics, where the error in the primitive sampling result becomes large. The error bars associated with the improved sampling remain small up until $t = 18$.

range of $[-1, 1]$.) The implementation of the improved sampling, however, reduces the error to the point where the dynamics can be accessed for three times as long a time period as that of the primitive sampling.

For the result displayed in Fig. 4.5, $\beta = 1.0$, $\Omega = 0.4$ and $\xi = 0.13$. This is still moderate coupling strength, but the temperature and energy level splitting has been increased. The two results are almost identical at short time, but after $= 10$ the statistical error for the primitive result grows, while the error in the improved sampling result stay small. This allows the dynamics to be accessed reliably for up to twice as long.

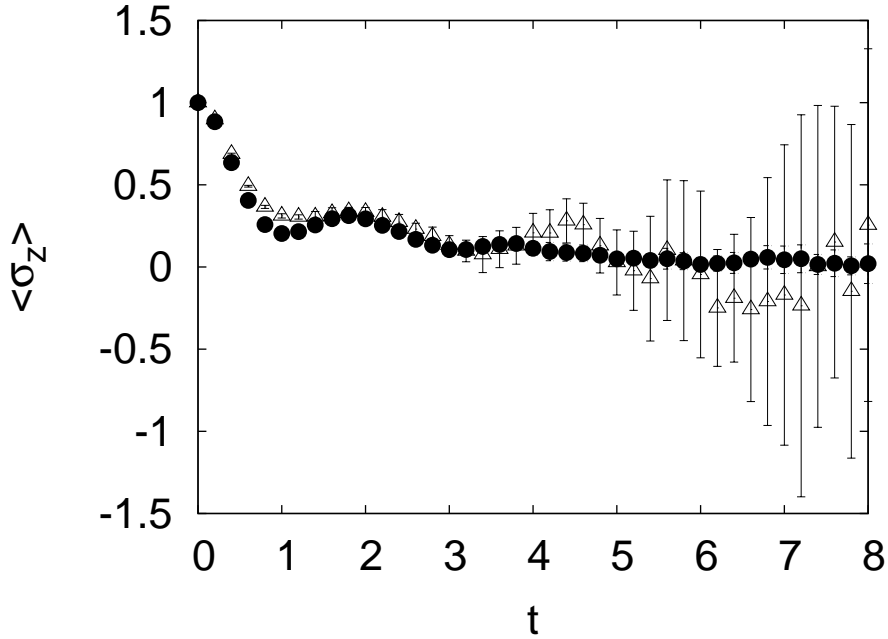Finally, I performed the calculation for the observable $\langle\sigma_z\rangle$ for strong

Figure 4.6: Comparison of the primitive ($\triangle$) and improved ($\bullet$) sampling schemes for the observable $\langle \sigma_z \rangle$ versus time. In this calculation, $\beta = 0.25$, $\Omega = 1.2$ and $\xi = 2.0$. Again, the optimum result was achieved using $c_{\mathcal{E}} = 0.1$. Two quantum transitions were included per trajectory. The error in the result for the primitive sampling grows large after $t = 5$, but the error for the improved sampling result remains scarcely bigger than the data points.

coupling between the subsystem and the bath. Dynamics for strong coupling is a problem for the SSTP algorithm, as the statistical error becomes great even at shorter times. In Fig. 4.6 the result is shown for $\beta = 0.25$, $\Omega = 1.2$ and $\xi = 2.0$. Only at short time (up to $t \approx 5$) does the primitive sampling scheme reliably simulate the dynamics. After this time, the statistical error grows very rapidly, and by $t = 7$ the error is greater than the possible range for $\langle \sigma_z \rangle$. Using a value for the numerical parameter $c_{\mathcal{E}} = 0.1$, this problem with the error is removed. The error bars are indistinguishable from the bullets up until $t = 6$, and at $t = 8$ they remain small.

4.4 Study of Momentum-Shift rules for Nonadiabatic Transitions

With the aim of formulating even more efficient sampling schemes, a more detailed study of momentum-shift rules for quantum transitions was performed in an attempt to discover what aspects are important in the rules. Any arbitrariness found can possibly be exploited to create an effective filtering scheme. Four different rules were studied by determining their effects on the results for the observable σ_z.

The first two rules have already been discussed in Chapter 3, namely the exact and approximate momentum-jump rules. It is instructive to determine whether the fact that one conserves the energy exactly, while the other does not, affects the result in any way. To indicate graphically the violation in energy conservation by the approximate momentum-jump rule, the energy for a single trajectory was monitored as a function of time. The result is shown in Fig. 4.7. The same was done for the exact momentum-jump rule, illustrating the fact that it conserves the energy (see Fig. 4.8).

Energy-Conserving Fictitious Momentum-Shift Rule

Consider the system in an $\alpha\alpha'$ state. The energy of the entire system is

$$E_{before} = \sum_{j=1}^{N} \frac{P_j^2}{2M} + \frac{1}{2}\left(E_\alpha + E_{\alpha'}\right) \; . \tag{4.38}$$

If the system undergoes an $\alpha \to \beta$ transition, the energy becomes

$$E_{after} = \sum_{j=1}^{N} \frac{(P_j + \Delta P_j)^2}{2M} + \frac{1}{2}\left(E_\beta + E_{\alpha'}\right) \; . \tag{4.39}$$

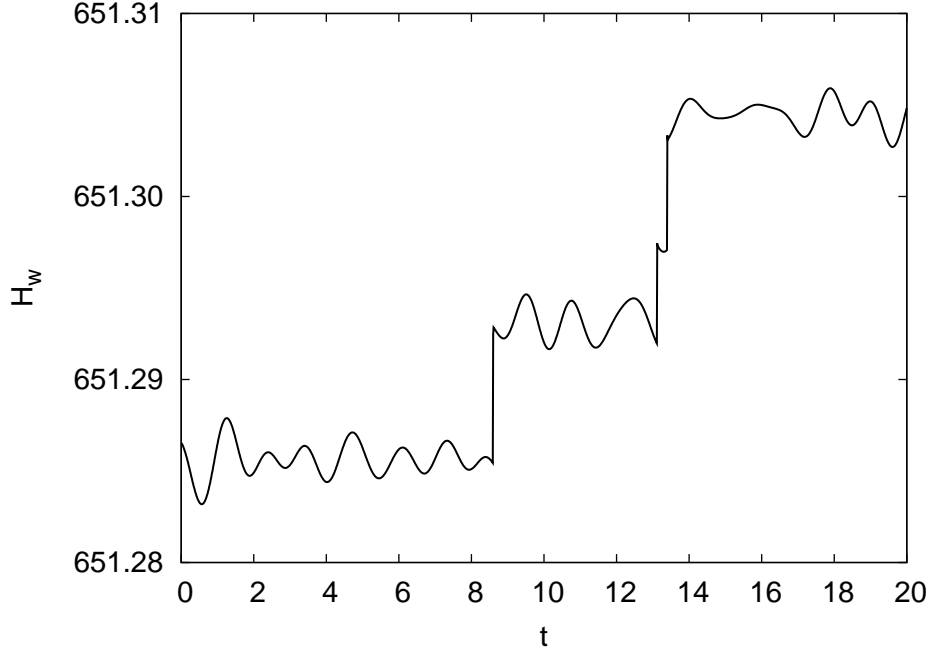Enforcing energy conservation requires that

Figure 4.7: A plot of the energy of a single trajectory versus time. This particular trajectory performed three nonadiabatic transitions. A jump in the energy approximately three times the average numerical fluctuation can be seen accompanying each transition, evidence that the approximate momentum-jump rule does indeed not conserve the energy of the system.

$$\sum_{j=1}^{N} \frac{P_j^2}{2M} + \frac{1}{2} \left(E_\alpha + E_{\alpha'}\right) = \sum_{j=1}^{N} \frac{(P_j + \Delta P_j)^2}{2M} + \frac{1}{2} \left(E_\beta + E_{\alpha'}\right) \ , \qquad (4.40)$$

$$\Rightarrow \Delta E_{\alpha\beta} = \sum_{j=1}^{N} \left[\frac{(P_j + \Delta P_j)^2}{M} - \frac{P_j^2}{M} \right] \ . \qquad (4.41)$$

where $\Delta E_{\alpha\beta} = E_\alpha - E_\beta$. Multiplying out, cancelling the P_j^2/M terms, and taking the $E_{\alpha\beta}$ term across gives

$$\sum_{j=1}^{N} \left[\Delta P_j^2 + 2P_j \Delta P_j - \frac{\Delta E_{\alpha\beta} M}{N} \right] = 0 \ . \qquad (4.42)$$

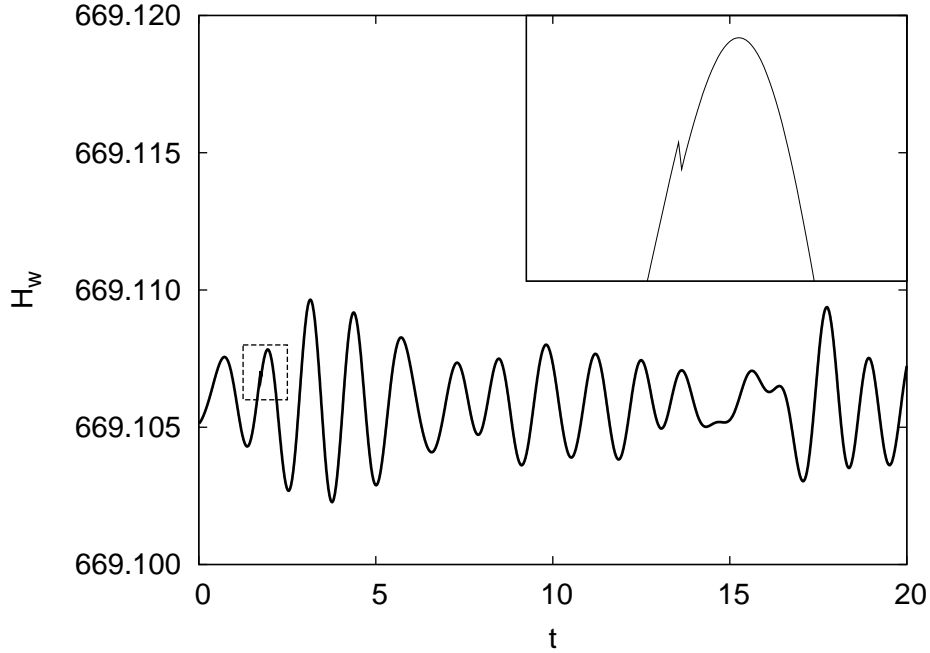Naturally, if the bath comprises more than one oscillator, there are in-

Figure 4.8: Plot of the energy of a single trajectory versus time. This trajectory performed two nonadiabatic transitions, at $t = 1.75$, and $t = 14.74$. As can be seen, there is essentially no change in the energy when a quantum transition occurs. Any change of energy accompanying a transition is roughly one hundredth of that of the average numerical fluctuation. The tiny variation of the energy for the transition at $t = 1.75$ is shown inset. This clearly demonstrates the energy conserving nature of the exact momentum-jump rule.

finitely many combinations of ΔP_j which satisfy Eq. (4.42). The simplest case is when all ΔP_j are the same. The ΔP_j are then given by the solutions to the quadratic equation $\Delta P_j^2 + 2P_j\Delta P_j - \Delta E_{\alpha\beta}M/N = 0$. That is,

$$\Delta P_j = -P_j + \sqrt{P_j^2 + \frac{\Delta E_{\alpha\beta}M}{N}} \ . \tag{4.43}$$

Only the solution with the positive square root is considered, as the negative square root would lead to a large change in the momentum, of the order $-2P_j$, as opposed to the smaller shift (4.43).

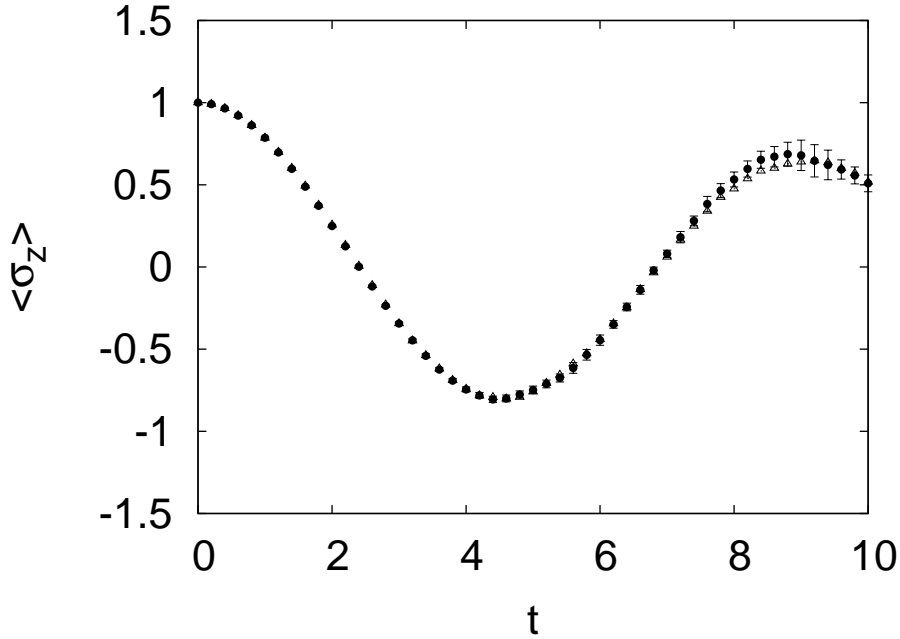Figure 4.9 displays the results for the population for the exact and ap-

Figure 4.9: Result for observable σ_z when using the exact momentum-shift rule ($\bullet$), and approximate rule ($\triangle$). The results are concordant despite the fact that only the exact rule conserves the energy.

proximate momentum shift rules. The results agree with each other almost exactly, indicating that to achieve good results the momentum-shift rule used does not necessarily have to conserve energy exactly. The next logical step would be to investigate whether the fact that a momentum-shift rule conserves the energy exactly implies that it gives good results. To this end, a third fictitious momentum-shift rule was derived directly from the stipulation of energy conservation, giving rise to Eq. (4.43). Numerical calculations for this momentum-shift rule were performed, and the results are compared in Fig. 4.10 with those of the exact rule.

The results were found to agree for only short times (up to $t \approx 4$), after which they begin to diverge. The fictitious rule is thus not a viable momentum-shift rule, even though it conserves the energy exactly.

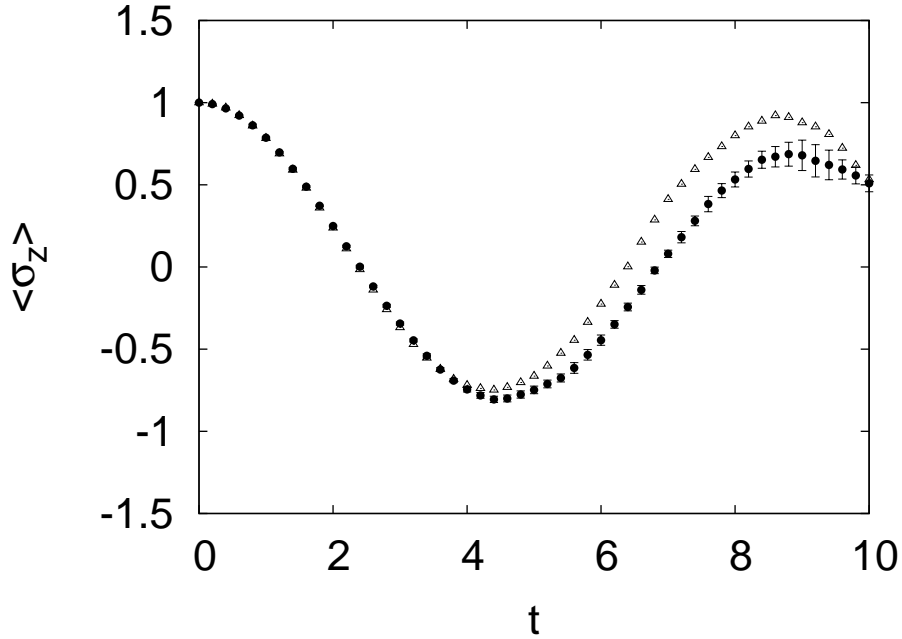There must therefore be something common to the exact and approxi-

Figure 4.10: Comparison of results for observable σ_z for the exact momentum-shift rule ($\bullet$), and the fictitious rule derived from energy conservation ($\triangle$). It is observed that the results only remain concordant before $t = 4$. After this time, the results begin to differ greatly, despite the fact that both rules exactly conserve the total energy of the system.

mate momentum-shift rules which is not included in the fictitious rule. This common trait is that in both exact and approximate rules, the quantum back reaction is taken along the nonadiabatic coupling vector $\hat{d}$.

With knowledge of the restrictions and areas of freedom in devising a viable momentum-shift scheme, it is hoped that even more efficient stochastic sampling schemes can be designed. This would help in the accessing of increasingly long times in nonadiabatic dynamics.

Chapter 5

Conclusions and Perspectives

One of the persisting problems in quantum computational physics is the inability to formulate any general algorithm to solve quantum dynamics of many-body interacting systems. The non-commuting algebra of quantum mechanics is very difficult to implement on the computer, and brute force methods for solving quantum systems is unrealistic as it generally demands far greater system resources than we currently possess. Because of the complexity involved in simulating quantum systems, approximations are made in such a way that the calculations become easier and algorithms developed can be faster and demand less computational resources. Quantum algorithms are generally devised to solve specific systems, and not for solving a diverse number of problems.

In the realm of classical numerical simulations we are generally far more able, with Molecular Dynamics or Monte Carlo methods being available to solve a wide variety of classical systems. This is what makes the quantum-classical approximation such a useful tool for modelling quantum systems. By treating the environment as classical, and only the subsystem of interest quantum mechanically, we are able to utilise many algorithms and techniques for solving classical dynamics, thereby making the problem much simpler computationally.

When considering systems where energy is free to be exchanged between the quantum subsystem and the classical bath, however, there are still nontrivial difficulties in implementing this numerically. Since the subsystem of interest is still quantum, there will be effects on the bath which are not classical in nature. More specifically, energy conservation requires that quantum transitions in the energy of the subsystem cause concomitant changes in the bath momentum. This remains a problem in numerical simulations, as methods used to implement this quantum back reaction cause large statistical error in the calculations. Solutions to these problems plaguing numerical quantum dynamics are of interest in a number of fields as computational simulations may give insights into the workings of many quantum systems. Within the last decade there has been a high level of interest in the new field of quantum biology [42]. In 2007, a paper published in *Nature* presented evidence that quantum coherent effects in photosynthesis cause the extremely efficient energy transfer observed in this biological process [43]. The numerical investigation of this phenomenon would naturally need algorithms for quantum dynamics, since there is no classical analogue for quantum coherence. Quantum-classical approximations may even be applied here, as the system comprises excitons interacting with an environment of proteins. Since the proteins are much more massive than the excitons, it is possible to treat them classically, while the exciton dynamics is still treated in a fully quantum way. It is with the long-term goal of being able to shed light on problems of interest such as these that my study was performed.

To summarise: the theory of nonadiabatic dynamics of quantum-classical systems was studied and discussed in detail. Focus was on the partial Wigner representation, leading to the quantum-classical Liouville equation. Surface-hopping algorithms, one of the most useful in simulating nonadiabatic quantum classical dynamics, which naturally arises from this formalism were examined. Specifically, sequential short-time propagation was used to perform

numerical studies of the spin-boson system, to better understand why such large error in the results occurs at long time.

In an effort to reduce this long-time error, an improved scheme for sampling nonadiabatic transitions was recently developed. This was based on the enforcement of energy conservation on the approximate momentum-shift rule arising from the momentum-jump approximation. I modified the sequential short-time propagation (SSTP) algorithm [27] to include this improved sampling scheme, and compared the results with simulations without the new sampling scheme. This was done for a range of system parameters hitherto not studied. As was shown, this improved scheme leads to a dramatic decrease in error in the results, compared to those of the old primitive scheme. The wide range of parameters used were chosen to show the efficacy of the improved sampling schemes [25].

I studied different momentum-shift rules used to numerically realise the quantum back reaction of the system on the bath accompanying a transition [26]. This was in an attempt to determine what constitutes a momentum-shift rule that will yield good numerical results. Any arbitrariness could be exploited in designing an even more efficient transition sampling scheme. It was found that exact energy conservation was firstly not a prerequisite to obtaining good numerical results, nor was it indicative of a good rule. The approximate momentum-shift rule was found to yield results just as accurate as those of the exact rule, even though its violation in energy conservation was of the order of three times the magnitude of the numerical fluctuation of the energy. A fictitious rule that was derived directly from energy conservation, however, gave results that only agreed with those of the exact momentum-shift rule at short times, after which it deviated. Comparison of the different rules implied that it is more important for a momentum-shift rule to take the quantum back reaction along the coupling vector d, than to conserve the energy exactly.

While we may attempt to reduce statistical error in numerical simulations by improving the sampling scheme utilised, there are other methods as well. Another area that can be improved upon is the short-time propagator in the algorithm. Recently, a new form for the time propagator derived using Trotter factorisation was shown to have greatly improved the accuracy of results [44], when compared with the SSTP algorithm. In fact, the method used is the same as that of the SSTP, which is to break up the propagator into small time segments. The major difference, however, is that the short-time propagator is more accurately approximated.

In future work, I plan to use this improved representation of the short-time propagator in conjunction with the improved sampling scheme, so that even greater times can be accessed reliably. In addition to this, I will continue my study of the various approximations used when simulating quantum-classical dynamics with the aim of devising even more effective sampling schemes.

Appendix A

Miscellaneous Derivations

A.1   The Heisenberg Equation of Motion

Writing the time dependence of the wave function explicitly, Eq. (2.1) becomes

$$\langle \chi(t) \rangle = \int \psi^*(x) e^{i\hat{H}t/\hbar} \hat{\chi} e^{-i\hat{H}t/\hbar} \psi(x) \, dx \; . \tag{A.1}$$

This allows us to define the time-dependent operator

$$\hat{\chi}(t) = e^{i\hat{H}t/\hbar} \hat{\chi} e^{-i\hat{H}t/\hbar} \; . \tag{A.2}$$

Taking the time derivative of this equation, we have

$$
\begin{aligned}
\frac{d\hat{\chi}(t)}{dt} &= \left(\frac{d}{dt} e^{i\hat{H}t/\hbar} \right) \hat{\chi} e^{-i\hat{H}t/\hbar} + e^{i\hat{H}t/\hbar} \left(\frac{\partial \hat{\chi}}{\partial t} \right) e^{-i\hat{H}t/\hbar} + e^{i\hat{H}t/\hbar} \hat{\chi} \left(\frac{d}{dt} e^{-i\hat{H}t/\hbar} \right) \\
&= \frac{i\hat{H}}{\hbar} e^{i\hat{H}t/\hbar} \hat{\chi} e^{-i\hat{H}t/\hbar} + \left(\frac{\partial \hat{\chi}}{\partial t} \right) + e^{i\hat{H}t/\hbar} \hat{\chi} \frac{-i\hat{H}}{\hbar} e^{-i\hat{H}t/\hbar} \\
&= \frac{i}{\hbar} \hat{H} \hat{\chi}(t) + \left(\frac{\partial \hat{\chi}}{\partial t} \right) - \frac{i}{\hbar} \hat{\chi}(t) \hat{H} \\
&= \frac{i}{\hbar} \left[\hat{H}, \hat{\chi}(t) \right] + \left(\frac{\partial \hat{\chi}}{\partial t} \right) \; .
\end{aligned}
\tag{A.3}
$$

A.2 Derivation of the Energy-Conserving Momentum-Jump Approximation Rule

We begin by approximating the J-operator with an exponential:

$$\left(1 + \frac{1}{2}\frac{\Delta E_{\alpha\beta}\hat{d}_{\alpha\beta}}{\frac{P}{M}\cdot\hat{d}_{\alpha\beta}}\cdot\frac{\partial}{\partial P}\right) \approx e^{\frac{1}{2}\frac{\Delta E_{\alpha\beta}\hat{d}_{\alpha\beta}}{\frac{P}{M}\cdot\hat{d}_{\alpha\beta}}\cdot\frac{\partial}{\partial P}} \ . \tag{A.4}$$

Using the chain rule on the momentum derivative, the argument of the exponential becomes

$$\frac{\Delta E_{\alpha\beta}\hat{d}_{\alpha\beta}}{2\frac{P}{M}\cdot\hat{d}_{\alpha\beta}}\cdot\frac{\partial}{\partial P} = \frac{\Delta E_{\alpha\beta}M}{2}\left[\frac{\hat{d}_{\alpha\beta}}{P\cdot\hat{d}_{\alpha\beta}}\right]\cdot\left[\frac{\partial}{\partial(P\cdot\hat{d}_{\alpha\beta})^2}\frac{\partial(P\cdot\hat{d}_{\alpha\beta})^2}{\partial P}\right] \ . \tag{A.5}$$

Now

$$\frac{\partial(P\cdot\hat{d}_{\alpha\beta})^2}{\partial P} = 2(P\cdot\hat{d}_{\alpha\beta})\hat{d}_{\alpha\beta} \ , \tag{A.6}$$

and since $\hat{d}_{\alpha\beta}$ is a unit vector, we have $\hat{d}_{\alpha\beta}\cdot\hat{d}_{\alpha\beta} = 1$. Hence, Eq. (A.5) reduces to

$$\frac{\Delta E_{\alpha\beta}\hat{d}_{\alpha\beta}}{2\frac{P}{M}\cdot\hat{d}_{\alpha\beta}}\cdot\frac{\partial}{\partial P} = \Delta E_{\alpha\beta}M\frac{\partial}{\partial(P\cdot\hat{d}_{\alpha\beta})^2} \ . \tag{A.7}$$

The J-operator acting on an arbitrary function of the bath momentum is now given (in addition to some multiplicative factors which are omitted here) by

$$\vec{J}\,f[P] = e^{\Delta E_{\alpha\beta}M\partial/\partial(P\cdot\hat{d}_{\alpha\beta})^2}f[P] \ . \tag{A.8}$$

If we resolve the bath momentum variable into its components along $\hat{d}_{\alpha\beta}$ and $\hat{d}_{\alpha\beta}^{\perp}$, the function of P can be rewritten as

$$
\begin{aligned}
f[P] &= f\left[\hat{d}^{\perp}_{\alpha\beta}(P \cdot \hat{d}^{\perp}_{\alpha\beta}) + \hat{d}_{\alpha\beta}(P \cdot \hat{d}_{\alpha\beta})\right] \\
&= f\left[\hat{d}^{\perp}_{\alpha\beta}(P \cdot \hat{d}^{\perp}_{\alpha\beta}) + \hat{d}_{\alpha\beta}sgn(P \cdot \hat{d}_{\alpha\beta})\sqrt{(P \cdot \hat{d}_{\alpha\beta})^2}\right] \ . \quad \text{(A.9)}
\end{aligned}
$$

We know from the identity given in Eq. (3.32) that the exponential in Eq. (A.8) acts by shifting the variable $\left(P \cdot \hat{d}\right)^2$ by an amount $\Delta E_{\alpha\beta}M$. We therefore have

$$
\begin{aligned}
&e^{\Delta E_{\alpha\beta}M\partial/\partial(P \cdot \hat{d}_{\alpha\beta})^2}f[P] \\
&= f\left[\hat{d}^{\perp}_{\alpha\beta}(P \cdot \hat{d}^{\perp}_{\alpha\beta}) + \hat{d}_{\alpha\beta}sgn(P \cdot \hat{d}_{\alpha\beta})\sqrt{(P \cdot \hat{d}_{\alpha\beta})^2 + \Delta E_{\alpha\beta}M}\right] \\
&= f\left[P - \hat{d}_{\alpha\beta}(P \cdot \hat{d}_{\alpha\beta}) + \hat{d}_{\alpha\beta}sgn(P \cdot \hat{d}_{\alpha\beta})\sqrt{(P \cdot \hat{d}_{\alpha\beta})^2 + \Delta E_{\alpha\beta}M}\right] \\
&= f\left[P + \Delta^{EMJ}P\right] \ . \quad\quad\quad\quad\quad\quad\quad\quad\quad\quad\quad\quad \text{(A.10)}
\end{aligned}
$$

The last line defines the formula for changing the momentum accompanying a quantum transition:

$$
\Delta^{EMJ}P_j = -\hat{d}_{\alpha\beta}(P \cdot \hat{d}_{\alpha\beta}) + \hat{d}_{\alpha\beta}sgn(P \cdot \hat{d}_{\alpha\beta})\sqrt{(P \cdot \hat{d}_{\alpha\beta})^2 + \Delta E_{\alpha\beta}M} \ . \quad \text{(A.11)}
$$

A.3 Proof of Energy Conservation for the EMJ rule

Consider an $\alpha \to \beta$ transition. The total energy of the spin-boson system before the transition occurs is

$$
E_{before} = \sum_j \frac{P_j^2}{2M} + \frac{1}{2}\left(E_\alpha + E_{\alpha'}\right) \ . \quad \text{(A.12)}
$$

The potential energy of the bath and the potential energy of coupling have

not been included in Eq. (A.12), as they are only dependent on the R coordinate. Since only the bath momentum changes accompanying a quantum transition, the potential energy of the system does not change during the transition. For energy to be conserved for the nonadiabatic transition, the energy of the system before must be equal to the energy afterwards, so

$$\sum_j \frac{P_j^2}{2M} + \frac{1}{2}\left(E_\alpha + E_{\alpha'}\right) = E_{after}$$
$$= \sum_j \frac{(P_j + \Delta P_j)^2}{2M} + \frac{1}{2}\left(E_\beta + E_{\alpha'}\right) . \text{(A.13)}$$

Multiplying both sides by 2 and cancelling the $E_{\alpha'}$ terms,

$$\sum_j \frac{P_j^2}{M} + (E_\alpha - E_\beta) = \sum_j \frac{(P_j + \Delta P_j)^2}{M}$$
$$= \sum_j \frac{P_j^2}{M} + \sum_j \frac{2P_j \Delta P_j}{M} + \sum_j \frac{(\Delta P_j)^2}{M} .$$
$$\text{(A.14)}$$

This gives the energy change in the subsystem for an $\alpha \to \beta$ transition in terms of the bath momentum and the changes in the bath momentum:

$$\Delta E_{\alpha\beta} = \sum_j \frac{2P_j \Delta P_j}{M} + \sum_j \frac{(\Delta P_j)^2}{M} . \tag{A.15}$$

Now substitute the exact momentum-jump rule for ΔP_j (Eq. A.11). It is easier to deal with each term separately, looking at the first term on the right-hand side:

$$\sum_j 2P_j \Delta P_j = \sum_j 2P_j \left[-\hat{d}_j \left(P \cdot \hat{d}\right) + \hat{d}_j sgn\left(P \cdot \hat{d}\right) \sqrt{\left(P \cdot \hat{d}\right)^2 + \Delta E_{\alpha\beta} M} \right]$$

$$= -2\left(P \cdot \hat{d}\right)^2 + 2\left(P \cdot \hat{d}\right) sgn\left(P \cdot \hat{d}\right) \sqrt{\left(P \cdot \hat{d}\right)^2 + \Delta E_{\alpha\beta} M} \, ,$$

$$(A.16)$$

where the fact that $\sum P_j \hat{d}_j = \left(P \cdot \hat{d}\right)$ and $\sqrt{\left(P \cdot \hat{d}\right)^2 + \Delta E_{\alpha\beta} M}$ and $\left(P \cdot \hat{d}\right)$ are constant over the summation has been used. The mass M is the same for all the bath coordinates, and can thus be taken out of the summation. Now for the second term:

$$
\begin{aligned}
\sum \left(\Delta P_j\right)^2 &= \sum_j \left[\left(P \cdot \hat{d}\right)^2 \hat{d}_j^2 - 2\hat{d}_j^2 \left(P \cdot \hat{d}\right) sgn\left(P \cdot \hat{d}\right) \right.\\
&\times \left. \sqrt{\left(P \cdot \hat{d}\right)^2 + \Delta E_{\alpha\beta} M} + \hat{d}_j^2 \left[\left(P \cdot \hat{d}\right)^2 + \Delta E_{\alpha\beta} M\right]\right]\\
&= \left(P \cdot \hat{d}\right)^2 - 2\left(P \cdot \hat{d}\right) sgn\left(P \cdot \hat{d}\right) \sqrt{\left(P \cdot \hat{d}\right)^2 + \Delta E_{\alpha\beta} M}\\
&+ \left(P \cdot \hat{d}\right)^2 + \Delta E_{\alpha\beta} M \, ,
\end{aligned}
$$

$$(A.17)$$

where the fact that $\sum \hat{d}_j^2 = \hat{d} \cdot \hat{d} = 1$ has been used. Eqs. A.16 and A.17 added together and multiplied by $1/M$ now yields

$$\sum_j \frac{2P_j \Delta P_j}{M} + \sum_j \frac{\left(\Delta P_j\right)^2}{M} = \Delta E_{\alpha\beta} \, .$$

$$(A.18)$$

This shows that the exact momentum-jump rule does indeed conserve the energy of the system.

Appendix B

Derivation of the quantum-classical Liouville superoperator in the Adiabatic Basis

This is a complete derivation of the one found in Ref. [2]. I performed this derivation as part of my study of the theory. Here I present the full derivation, including the steps not shown in the reference given above.

The first step is to take the matrix elements of the quantum-classical Liouville equation for the density matrix -

$$
\begin{aligned}
\langle\alpha|\frac{\partial\rho_W}{\partial t}|\alpha'\rangle &= -\frac{i}{\hbar}\langle\alpha|\left[\hat{H}_W,\hat{\rho}_W\right]|\alpha'\rangle + \frac{1}{2}\langle\alpha|\{\hat{H}_W,\hat{\rho}_W\}|\alpha'\rangle \\
&\quad - \frac{1}{2}\langle\alpha|\{\hat{\rho}_W,\hat{H}_W\}|\alpha'\rangle,
\end{aligned} \tag{B.1}
$$

where $\{..,..\}$ denotes the classical Poisson bracket. Expand the first term on the right-hand side:

$$\langle\alpha|\left[\hat{H}_W,\hat{\rho}_W\right]|\alpha'\rangle = -\frac{i}{\hbar}\left[\langle\alpha|\hat{H}_W\hat{\rho}_W|\alpha'\rangle - \langle\alpha|\hat{\rho}_W\hat{H}_W|\alpha'\rangle\right] . \qquad \text{(B.2)}$$

Now using the fact that $\hat{H}_W = P^2/2M + \hat{h}_W$, and $\hat{h}_W|\alpha\rangle = E_\alpha|\alpha\rangle$, this becomes

$$
\begin{aligned}
\frac{i}{\hbar}\left[\langle\alpha|\hat{H}_W\hat{\rho}_W|\alpha'\rangle - \langle\alpha|\hat{\rho}_W\hat{H}_W|\alpha'\rangle\right] &= -\frac{i}{\hbar}\left[E_\alpha\langle\alpha|\hat{\rho}_W|\alpha'\rangle - E_{\alpha'}\langle\alpha|\hat{\rho}_W|\alpha'\rangle\right] \\
&= -i\omega_{\alpha\alpha'}\rho_W^{\alpha\alpha'} , \qquad\qquad \text{(B.3)}
\end{aligned}
$$

where $\langle\alpha|\hat{\rho}_W|\alpha'\rangle = \rho_W^{\alpha\alpha'}$. The second term of Eq. (B.1) can now be expanded as well:

$$\langle\alpha|\{\hat{H}_W,\hat{\rho}_W\}|\alpha'\rangle = \langle\alpha|\frac{\partial\hat{H}_W}{\partial R}\frac{\partial\hat{\rho}_W}{\partial P}|\alpha'\rangle - \langle\alpha|\frac{\partial\hat{H}_W}{\partial P}\frac{\partial\hat{\rho}_W}{\partial R}|\alpha'\rangle . \qquad \text{(B.4)}$$

Using the completeness relation, this becomes

$$
\begin{aligned}
\langle\alpha|\{\hat{H}_W,\hat{\rho}_W\}|\alpha'\rangle &= \langle\alpha|\frac{\partial\hat{H}_W}{\partial R}\sum_\beta|\beta\rangle\langle\beta|\frac{\partial\hat{\rho}_W}{\partial P}|\alpha'\rangle \\
&\quad -\langle\alpha|\frac{\partial\hat{H}_W}{\partial P}\sum_\beta|\beta\rangle\langle\beta|\frac{\partial\hat{\rho}_W}{\partial R}|\alpha'\rangle \\
&= -\sum_\beta F_W^{\alpha\beta}\frac{\partial\rho_W^{\beta\alpha'}}{\partial P} - \sum_\beta\frac{P}{M}\delta_{\alpha\beta}\langle\beta|\frac{\partial\hat{\rho}_W}{\partial R}|\alpha'\rangle ,
\end{aligned}
$$
$$\text{(B.5)}$$

where the fact that $\langle\alpha|\beta\rangle = \delta_{\alpha\beta}$ has been used, as well as $\partial\hat{H}_W/\partial R = \partial\hat{V}_W/\partial R$ and $\partial\hat{H}_W/\partial P = P/M$. The Hellmann-Feynman matrix elements in the partial Wigner representation are given by

$$F_W^{\alpha\beta} = -\langle\alpha|\frac{\partial\hat{V}_W}{\partial R}|\beta\rangle . \qquad \text{(B.6)}$$

The third term in Eq. (B.1) can be similarly expanded to yield

$$\langle\alpha|\{\hat{\rho}_W, \hat{H}_W\}|\alpha'\rangle = \sum_\beta \langle\alpha|\frac{\partial\hat{\rho}_W}{\partial R}|\beta\rangle\frac{P}{M}\delta_{\alpha'\beta} + \sum_\beta \frac{\partial\rho_W^{\alpha\beta}}{\partial P}F_W^{\beta\alpha'} \ . \qquad (B.7)$$

Adding equations (B.3), (B.5) and (B.7) gives

$$
\begin{aligned}
\frac{\partial\rho_W^{\alpha\alpha'}}{\partial t} &= -i\omega_{\alpha\alpha'}\rho_W^{\alpha\alpha'} - \frac{1}{2}\sum_\beta \left(F_W^{\alpha\beta}\frac{\partial\rho_W^{\beta\alpha'}}{\partial P} + \frac{\partial\rho_W^{\alpha\beta}}{\partial P}F_W^{\beta\alpha'} \right) \\
&\quad - \frac{1}{2}\sum_\beta \left(\frac{P}{M}\langle\alpha|\frac{\partial\hat{\rho}_W}{\partial R}|\beta\rangle\delta_{\alpha\beta} + \frac{P}{M}\langle\beta|\frac{\partial\hat{\rho}_W}{\partial R}|\alpha'\rangle \right) \\
&= -i\omega_{\alpha\alpha'}\rho_W^{\alpha\alpha'} - \frac{1}{2}\sum_\beta \left(F_W^{\alpha\beta}\frac{\partial\rho_W^{\beta\alpha'}}{\partial P} + \frac{\partial\rho_W^{\alpha\beta}}{\partial P}F_W^{\beta\alpha'} \right) \\
&\quad - \frac{P}{M}\langle\alpha|\frac{\partial\hat{\rho}_W}{\partial R}|\alpha'\rangle \ .
\end{aligned}
\qquad (B.8)
$$

The term on the last line of the above equation can not be written simply as $\frac{P}{M}\frac{\partial\rho_W^{\alpha\alpha'}}{\partial R}$, since the adiabatic basis states are dependent on the bath position coordinate R. We thus consider

$$
\begin{aligned}
\frac{\partial}{\partial R}\langle\alpha|\hat{\rho}_W|\alpha'\rangle &= \langle\frac{\partial\alpha}{\partial R}|\hat{\rho}_W|\alpha'\rangle + \langle\alpha|\frac{\partial\hat{\rho}_W}{\partial R}|\alpha'\rangle + \langle\alpha|\hat{\rho}_W|\frac{\partial\alpha'}{\partial R}\rangle \\
&= \langle\frac{\partial\alpha}{\partial R}|\sum_\beta |\beta\rangle\langle\beta|\hat{\rho}_W|\alpha'\rangle + \langle\alpha|\frac{\partial\hat{\rho}_W}{\partial R}|\alpha'\rangle \\
&\quad + \langle\alpha|\hat{\rho}_W\sum_\beta |\beta\rangle\langle\beta|\frac{\partial\alpha'}{\partial R}\rangle \\
&= \langle\alpha|\frac{\partial\hat{\rho}_W}{\partial R}|\alpha'\rangle + \sum_\beta \left(\langle\frac{\partial\alpha}{\partial R}|\beta\rangle\rho_W^{\beta\alpha'} + \rho_W^{\alpha\beta}\langle\beta|\frac{\partial\alpha'}{\partial R}\rangle \right) \ ,
\end{aligned}
\qquad (B.9)
$$

where the completeness relation has again been used. We know that, by definition, $\langle\beta|\frac{\partial\alpha'}{\partial R}\rangle = \langle\beta|\frac{\partial}{\partial R}|\alpha'\rangle = d_{\beta\alpha'}$, but to simplify the term $\langle\frac{\partial\alpha}{\partial R}|\beta\rangle$, we must consider

$$\frac{\partial}{\partial R}\langle\alpha|\beta\rangle = 0 \ . \qquad (B.10)$$

This is obviously true, since $\langle \alpha | \beta \rangle = \delta_{\alpha\beta}$. But

$$\frac{\partial}{\partial R} \langle \alpha | \beta \rangle = \langle \frac{\partial \alpha}{\partial R} | \beta \rangle + \langle \alpha | \frac{\partial \beta}{\partial R} \rangle \ . \tag{B.11}$$

We thus obtain the identity

$$\begin{aligned} \langle \frac{\partial \alpha}{\partial R} | \beta \rangle &= -\langle \alpha | \frac{\partial \beta}{\partial R} \rangle \\ &= -d_{\alpha\beta} \ . \end{aligned} \tag{B.12}$$

Using this identity in Eq. (B.9), and rearranging to make $\langle \alpha | \frac{\partial \hat{\rho}_W}{\partial R} | \alpha' \rangle$ the subject of the formula now gives

$$\langle \alpha | \frac{\partial \hat{\rho}_W}{\partial R} | \alpha' \rangle = \frac{\partial \rho_W^{\alpha\alpha'}}{\partial R} - \sum_\beta \left(\rho_W^{\alpha\beta} d_{\beta\alpha'} - d_{\alpha\beta} \rho_W^{\beta\alpha'} \right) \ . \tag{B.13}$$

Substituting this expression for $\langle \alpha | \frac{\partial \hat{\rho}_W}{\partial R} | \alpha' \rangle$ back into Eq. (B.8), we arrive at the following equation for the time derivative of the density matrix elements:

$$\begin{aligned} \frac{\partial \rho_W^{\alpha\alpha'}(R,P,t)}{\partial t} &= -i\omega_{\alpha\alpha'} \rho_W^{\alpha\alpha'} - \frac{1}{2} \sum_\beta \left(F_W^{\alpha\beta} \frac{\partial \rho_W^{\beta\alpha'}}{\partial P} + \frac{\partial \rho_W^{\alpha\beta}}{\partial P} F_W^{\beta\alpha'} \right) \\ &\quad - \frac{P}{M} \frac{\partial \rho_W^{\alpha\alpha'}}{\partial R} + \frac{P}{M} \sum_\beta \left(\rho_W^{\alpha\beta} d_{\beta\alpha'} - d_{\alpha\beta} \rho_W^{\beta\alpha'} \right) \\ &= \sum_{\beta\beta'} \left[-i\omega_{\alpha\alpha'} \delta_{\alpha\beta} \delta_{\alpha'\beta} - \frac{1}{2} \left(F_W^{\alpha\beta} \delta_{\alpha'\beta'} \frac{\partial}{\partial P} + F_W^{\beta'\alpha'} \delta_{\alpha\beta} \frac{\partial}{\partial P} \right) \right. \\ &\quad \left. - \frac{P}{M} \delta_{\alpha\beta} \delta_{\alpha'\beta'} \frac{\partial}{\partial R} + \frac{P}{M} \left(d_{\beta'\alpha'} \delta_{\alpha\beta} - d_{\alpha\beta} \delta_{\alpha'\beta'} \right) \right] \rho_W^{\beta\beta'}(R,P,t) \\ &= \sum_{\beta\beta'} -i\mathcal{L}_{\alpha\alpha',\beta\beta'} \rho_W^{\beta\beta'}(R,P,t) \ . \tag{B.14} \end{aligned}$$

In the last line of the above equation, the quantum-classical Liouville superoperator has been defined. Now we wish to cast it in the form given in Eq. (3.10). We first define the Liouville operator [2]

$$iL_{\alpha\alpha'} = \frac{P}{M} \frac{\partial}{\partial R} + \frac{1}{2} \left(F_W^{\alpha} + F_W^{\alpha'} \right) \frac{\partial}{\partial P} \ . \tag{B.15}$$

This operator describes the classical evolution of the bath coordinates, and is given in terms of the Hellmann-Feynman forces for the adiabatic states α and α' [34]. The quantum-classical Liouville superoperator can now be written in the form

$$
\begin{aligned}
-i\mathcal{L}_{\alpha\alpha',\beta\beta'} &= -(i\omega_{\alpha\alpha'} + iL_{\alpha\alpha'})\delta_{\alpha\beta}\delta_{\alpha'\beta'} + \left[\frac{P}{M}\left(d_{\beta'\alpha'}\delta_{\alpha\beta} - d_{\alpha\beta}\delta_{\alpha'\beta'}\right) \right. \\
&\quad - \left. \frac{1}{2}\left(F_W^{\alpha\beta}\delta_{\alpha'\beta'} + F_W^{\beta'\alpha'}\delta_{\alpha\beta} - (F_W^{\alpha} + F_W^{\alpha'})\delta_{\alpha\beta}\delta_{\alpha'\beta'}\right)\frac{\partial}{\partial P} \right] .
\end{aligned}
$$
(B.16)

The terms in the square brackets are the operator $J_{\alpha\alpha',\beta\beta'}$. We now wish to obtain from these terms, the form for the J-operator given by Eq. (3.13). The first step is to group all the terms with a coefficient $\delta_{\alpha'\beta'}$ together, and all the terms with a coefficient $\delta_{\alpha\beta}$ together, to give

$$
\begin{aligned}
J_{\alpha\alpha',\beta\beta'} &= \left[-\frac{P}{M}d_{\alpha\beta} - \frac{1}{2}\left(F_W^{\alpha\beta} - F_W^{\alpha}\delta_{\alpha\beta}\right)\frac{\partial}{\partial P} \right]\delta_{\alpha'\beta'} \\
&\quad + \left[\frac{P}{M}d_{\beta'\alpha'} - \frac{1}{2}\left(F_W^{\beta'\alpha'} - F_W^{\alpha'}\delta_{\alpha'\beta'}\right)\frac{\partial}{\partial P} \right]\delta_{\alpha\beta} .
\end{aligned}
$$
(B.17)

Now consider the derivative with respect to the bath position coordinate R, of the matrix elements of the Hamiltonian:

$$
\begin{aligned}
-\frac{\partial}{\partial R}\langle\alpha|\hat{H}_W|\beta\rangle &= -\langle\frac{\partial\alpha}{\partial R}|\hat{H}_W|\beta\rangle - \langle\alpha|\frac{\partial\hat{H}_W}{\partial R}|\beta\rangle - \langle\alpha|\hat{H}_W|\frac{\partial\beta}{\partial R}\rangle \\
&= -\langle\frac{\partial\alpha}{\partial R}|\left(\frac{P^2}{2M} + \hat{h}_W\right)|\beta\rangle - \langle\alpha|\left(\frac{\partial}{\partial R}\left(\frac{P^2}{2M} + \hat{h}_W\right)\right)|\beta\rangle \\
&\quad -\langle\alpha|\left(\frac{P^2}{2M} + \hat{h}_W\right)|\frac{\partial\beta}{\partial R}\rangle \\
&= \langle\alpha|\frac{\partial}{\partial R}\hat{h}_W|\beta\rangle - \langle\alpha|\left(\frac{\partial\hat{h}_W}{\partial R}\right)|\beta\rangle - \langle\alpha|\hat{h}_W\frac{\partial}{\partial R}|\beta\rangle .
\end{aligned}
$$
(B.18)

The bath kinetic energy terms all disappear because $\partial P/\partial R = 0$. Using

$\langle\alpha|\hat{h}_W = E_\alpha,\ \hat{h}_W|\beta\rangle = E_\beta$, and $-\langle\alpha|\left(\frac{\partial\hat{h}_W}{\partial R}\right)|\beta\rangle = F_W^{\alpha\beta}$, the above equation becomes

$$
\begin{aligned}
-\frac{\partial}{\partial R}\langle\alpha|\hat{H}_W|\beta\rangle &= E_\beta\langle\alpha|\frac{\partial}{\partial R}|\beta\rangle + F_W^{\alpha\beta} - E_\alpha\langle\alpha|\frac{\partial}{\partial R}|\beta\rangle \\
&= F_W^{\alpha\beta} - (E_\alpha - E_\beta)\,d_{\alpha\beta}\ . \quad\quad\quad \text{(B.19)}
\end{aligned}
$$

But

$$
\begin{aligned}
-\frac{\partial}{\partial R}\langle\alpha|\hat{H}_W|\beta\rangle &= -\frac{\partial}{\partial R}\left[\langle\alpha|\frac{P^2}{2M}|\beta\rangle + \langle\alpha|\hat{h}_W|\beta\rangle\right] \\
&= -\frac{\partial}{\partial R}E_\beta\delta_{\alpha\beta} \\
&= F_W^\beta\delta_{\alpha\beta} = F_W^\alpha\delta_{\alpha\beta}\ . \quad\quad\quad \text{(B.20)}
\end{aligned}
$$

If we substitute this expression for $-\frac{\partial}{\partial R}\langle\alpha|\hat{H}_W|\beta\rangle$ back into Eq. (B.19), we obtain the identity

$$
F_W^{\alpha\beta} - F_W^\alpha\delta_{\alpha\beta} = (E_\alpha - E_\beta)d_{\alpha\beta}\ . \quad\quad\quad \text{(B.21)}
$$

Upon use of this identity, Eq (B.17) becomes

$$
\begin{aligned}
J_{\alpha\alpha',\beta\beta'} &= \left[-\frac{P}{M}d_{\alpha\beta} - \frac{1}{2}\left(E_\alpha - E_\beta\right)d_{\alpha\beta}\frac{\partial}{\partial P}\right]\delta_{\alpha'\beta'} \\
&+ \left[\frac{P}{M}d_{\beta'\alpha'} + \frac{1}{2}\left(E_\alpha - E_{\beta'}\right)d_{\beta'\alpha'}\frac{\partial}{\partial P}\right]\delta_{\alpha\beta}\ . \quad\quad \text{(B.22)}
\end{aligned}
$$

Note that $d_{\beta'\alpha'} = -d^*_{\alpha'\beta}$, since the matrix for the nonadiabatic coupling vector is anti-hermitian. Making this substitution for $d_{\beta'\alpha'}$, and taking out common factors of $-d_{\alpha\beta}P/M$ and $-d_{\alpha'\beta'}P/M$ from the first and second pair of square brackets respectively, gives

$$J_{\alpha\alpha',\beta\beta'} = \; - \; \frac{P}{M} \cdot d_{\alpha\beta} \left(1 + \frac{1}{2} \frac{\Delta E_{\alpha\beta} d_{\alpha\beta}}{\frac{P}{M} \cdot d_{\alpha\beta}} \frac{\partial}{\partial P} \right) \delta_{\alpha'\beta'}$$

$$- \; \frac{P}{M} d^{*}_{\alpha'\beta'} \left(1 + \frac{1}{2} \frac{\Delta E_{\alpha\beta} d^{*}_{\alpha'\beta}}{\frac{P}{M} \cdot d^{*}_{\alpha'\beta'}} \frac{\partial}{\partial P} \right) \delta_{\alpha\beta} \;, \qquad \text{(B.23)}$$

which is the form for the J-operator given in Eq. (3.13).

Appendix C

Derivation of the bath phase-space distribution function

Here is the complete derivation for the distribution function for a canonical ensemble of harmonic oscillators. This derivation can be found in [45]. I performed and checked this derivation as part of my study of the theory.

Consider the canonical ensemble. The density matrix is given by

$$\hat{\rho} = \frac{1}{Z(\beta)} e^{-\beta \hat{H}} \equiv \frac{1}{Z(\beta)} \hat{\Omega} \, , \tag{C.1}$$

where $\beta = 1/kT$, with k being the Boltzmann constant, and $Z(\beta) = Tr\left(e^{-\beta \hat{H}}\right)$ is the canonical partition function. If the initial condition $\hat{\Omega}(\beta = 0) = \hat{I}$ is satisfied, where $\hat{I}$ is the identity matrix, then the unnormalised density matrix satisfies the Bloch equation -

$$\frac{\partial \hat{\Omega}}{\partial \beta} = -\hat{H}\hat{\Omega}$$

$$= -\hat{\Omega}\hat{H} \ . \tag{C.2}$$

If we apply the Wigner transform, using the identity given in Eq. (2.32), this equation becomes:

$$
\begin{aligned}
\frac{\partial \Omega_W(q,p)}{\partial \beta} &= -H_W(q,p)e^{\frac{\hbar\Lambda}{2i}}\Omega_W(q,p) \\
&= -\Omega_W(q,p)e^{\frac{\hbar\Lambda}{2i}}H_W(q,p) \ ,
\end{aligned}
\tag{C.3}
$$

where Λ is the negative of the Poisson bracket and (q,p) are phase-space coordinates. Using Eq. (C.3) and Eq. (2.32), we find that

$$H_W(q,p)e^{\frac{\hbar\Lambda}{2i}}\Omega_W(q,p) = H_W(q,p)e^{-\frac{\hbar\Lambda}{2i}}\Omega_W(q,p) \ . \tag{C.4}$$

Therefore, the Wigner transformed Bloch equation can be rewritten as

$$\frac{\partial \Omega_W(q,p)}{\partial \beta} = \frac{1}{2}\left[-H_W(q,p)e^{\frac{\hbar\Lambda}{2i}}\Omega_W(q,p) - H_W(q,p)e^{-\frac{\hbar\Lambda}{2i}}\Omega_W(q,p)\right] \ . \tag{C.5}$$

Using the Euler formula,

$$
\begin{aligned}
\frac{\partial \Omega_W(q,p)}{\partial \beta} &= \frac{1}{2}\left[-H_W\left(\cos\left(\frac{\hbar\Lambda}{2}\right) - i\sin\left(\frac{\hbar\Lambda}{2}\right)\right)\Omega_W \right.\\
&\quad - \left. H_W\left(\cos\left(\frac{\hbar\Lambda}{2}\right) + i\sin\left(\frac{\hbar\Lambda}{2}\right)\right)\Omega_W\right] \\
&= -H_W(q,p)\cos\left(\frac{\hbar\Lambda}{2}\right)\Omega_W(q,p) \ .
\end{aligned}
\tag{C.6}
$$

Consider now a harmonic Hamiltonian

$$H_W = \frac{p^2}{2m} + \frac{1}{2}m\omega^2 q^2 \ . \tag{C.7}$$

The Wigner transformed Bloch equation for this Hamiltonian is

$$\frac{\partial \Omega_W}{\partial \beta} = -\left(\frac{p^2}{2m} + \frac{1}{2}m\omega^2 q^2\right) \cos\left(\frac{\hbar}{2}\left[\frac{\overleftarrow{\partial}}{\partial q}\frac{\overrightarrow{\partial}}{\partial p} - \frac{\overleftarrow{\partial}}{\partial p}\frac{\overrightarrow{\partial}}{\partial q}\right]\right)\Omega_W .\qquad \text{(C.8)}$$

We expand the cosine term to second order:

$$\cos\left(\frac{\hbar}{2}\left(\frac{\overleftarrow{\partial}}{\partial q}\frac{\overrightarrow{\partial}}{\partial p} - \frac{\overleftarrow{\partial}}{\partial p}\frac{\overrightarrow{\partial}}{\partial q}\right)\right) = 1 - \frac{1}{2}\left(\frac{\hbar}{2}\right)^2\left(\frac{\overleftarrow{\partial}}{\partial q}\frac{\overrightarrow{\partial}}{\partial p} - \frac{\overleftarrow{\partial}}{\partial p}\frac{\overrightarrow{\partial}}{\partial q}\right)^2 .\qquad \text{(C.9)}$$

Multiplying out the derivatives term gives

$$
\begin{aligned}
\left(\frac{\overleftarrow{\partial}}{\partial q}\frac{\overrightarrow{\partial}}{\partial p} - \frac{\overleftarrow{\partial}}{\partial p}\frac{\overrightarrow{\partial}}{\partial q}\right)^2 &= \frac{\overleftarrow{\partial}}{\partial q}\frac{\overrightarrow{\partial}}{\partial p}\frac{\overleftarrow{\partial}}{\partial q}\frac{\overrightarrow{\partial}}{\partial p} - \frac{\overleftarrow{\partial}}{\partial q}\frac{\overrightarrow{\partial}}{\partial p}\frac{\overleftarrow{\partial}}{\partial p}\frac{\overrightarrow{\partial}}{\partial q} \\
&\quad - \frac{\overleftarrow{\partial}}{\partial p}\frac{\overrightarrow{\partial}}{\partial q}\frac{\overleftarrow{\partial}}{\partial q}\frac{\overrightarrow{\partial}}{\partial p} + \frac{\overleftarrow{\partial}}{\partial p}\frac{\overrightarrow{\partial}}{\partial q}\frac{\overleftarrow{\partial}}{\partial p}\frac{\overrightarrow{\partial}}{\partial q} \\
&= \frac{\overleftarrow{\partial^2}}{\partial q^2}\frac{\overrightarrow{\partial^2}}{\partial p^2} - \frac{\overleftarrow{\partial^2}}{\partial q\partial p}\frac{\overrightarrow{\partial^2}}{\partial q\partial p} - \frac{\overleftarrow{\partial^2}}{\partial p\partial q}\frac{\overrightarrow{\partial^2}}{\partial q\partial p} \\
&\quad + \frac{\overleftarrow{\partial^2}}{\partial p^2}\frac{\overrightarrow{\partial^2}}{\partial q^2} \\
&= \frac{\overleftarrow{\partial^2}}{\partial q^2}\frac{\overrightarrow{\partial^2}}{\partial p^2} - 2\frac{\overleftarrow{\partial^2}}{\partial q\partial p}\frac{\overrightarrow{\partial^2}}{\partial q\partial p} + \frac{\overleftarrow{\partial^2}}{\partial p^2}\frac{\overrightarrow{\partial^2}}{\partial q^2} .\ \text{(C.10)}
\end{aligned}
$$

If we substitute this second order expression for the cosine term into Eq. (C.8), we obtain

$$
\begin{aligned}
\frac{\partial \Omega_W}{\partial \beta} &= -\frac{p^2}{2m}\left[1 - \frac{\hbar^2}{8}\left(\frac{\overleftarrow{\partial^2}}{\partial q^2}\frac{\overrightarrow{\partial^2}}{\partial p^2} - 2\frac{\overleftarrow{\partial^2}}{\partial q\partial p}\frac{\overrightarrow{\partial^2}}{\partial q\partial p} + \frac{\overleftarrow{\partial^2}}{\partial p^2}\frac{\overrightarrow{\partial^2}}{\partial q^2}\right)\right]\Omega_W \\
&\quad - \frac{m\omega^2 q^2}{2}\left[1 - \frac{\hbar^2}{8}\left(\frac{\overleftarrow{\partial^2}}{\partial q^2}\frac{\overrightarrow{\partial^2}}{\partial p^2} - 2\frac{\overleftarrow{\partial^2}}{\partial q\partial p}\frac{\overrightarrow{\partial^2}}{\partial q\partial p} + \frac{\overleftarrow{\partial^2}}{\partial p^2}\frac{\overrightarrow{\partial^2}}{\partial q^2}\right)\right]\Omega_W
\end{aligned}
$$

$$= -\left(\frac{p^2}{2m} - \frac{1}{2}m\omega^2 q^2\right)\Omega_W + \frac{\hbar^2}{8m}\frac{\partial^2\Omega_W}{\partial q^2} + \frac{\hbar^2}{8}m\omega^2\frac{\partial^2\Omega_W}{\partial p^2} \ .$$

$$\text{(C.11)}$$

This is the Wigner transformed Bloch equation for the harmonic oscillator. The second order approximation for the cosine term is exact for harmonic Hamiltonians, as higher order terms only contain derivatives of order higher than two, which, when acting on the Hamiltonian, yield zero.

The above equation is difficult to solve as it stands, so we make the ansatz

$$\Omega_W(q,p) = e^{-A(\beta)H_W + B(\beta)} \ , \tag{C.12}$$

where A and B are subject to the initial conditions $A(0) = B(0) = 0$. Now we determine the derivatives of Ω_W with respect to the spatial coordinate:

$$\frac{\partial\Omega_W}{\partial q} = \Omega_W\left(-A(\beta)\frac{\partial H_W}{\partial q}\right) \ ,$$

and hence

$$\begin{aligned}
\frac{\partial^2\Omega_W}{\partial q^2} &= \frac{\partial\Omega_W}{\partial q}\left(-A(\beta)\frac{\partial H_W}{\partial q}\right) - A(\beta)\Omega_W\frac{\partial^2 H_W}{\partial q^2} \\
&= \left(-A(\beta)\frac{\partial H_W}{\partial q}\right)^2\Omega_W - A(\beta)\Omega_W\frac{\partial^2 H_W}{\partial q^2} \\
&= \left(A^2(\beta)m^2\omega^4 q^2 - A(\beta)m\omega^2\right)\Omega_W \ . \tag{C.13}
\end{aligned}$$

Similarly, with respect to the momentum coordinate:

$$\frac{\partial\Omega_W}{\partial p} = -A(\beta)\frac{\partial H_W}{\partial p}\Omega_W \ ,$$

and hence

$$
\begin{aligned}
\frac{\partial^2 \Omega_W}{\partial p^2} &= -A(\beta)\frac{\partial^2 H_W}{\partial p^2}\Omega_W - A(\beta)\frac{\partial H_W}{\partial p}\frac{\partial \Omega_W}{\partial p} \\
&= -A(\beta)\frac{\partial^2 H_W}{\partial p^2}\Omega_W + \left(A(\beta)\frac{\partial H_W}{\partial p}\right)^2 \\
&= -\frac{A(\beta)}{m}\Omega_W + \left(A(\beta)\frac{p}{m}\right)^2 \Omega_W \\
&= -\frac{A(\beta)}{m}\Omega + A^2(\beta)\frac{p^2}{m^2}\Omega_W \ . \quad\quad\text{(C.14)}
\end{aligned}
$$

And finally, with respect to β:

$$
\frac{\partial \Omega_W}{\partial \beta} = \left(-\frac{\partial A}{\partial \beta}H_W + \frac{\partial B}{\partial \beta}\right)\Omega_W \ .
$$

The Wigner transformed Bloch equation thus becomes

$$
\begin{aligned}
\left(-\frac{\partial A}{\partial \beta}H_W + \frac{\partial B}{\partial \beta}\right)\Omega_W &= -\left(\frac{p^2}{2m} + \frac{1}{2}m\omega^2 q^2\right)\Omega_W \\
&\quad + \frac{\hbar^2}{8}\left(\frac{1}{m}\frac{\partial^2 \Omega_W}{\partial q^2} + m^2\omega^2\frac{\partial^2 \Omega_W}{\partial p^2}\right) \ . \quad\text{(C.15)}
\end{aligned}
$$

Now

$$
\begin{aligned}
\frac{\hbar^2}{8m}\left(\frac{\partial^2 \Omega_W}{\partial q^2}\right) &= \frac{\hbar^2}{8m}(A^2 m^2\omega^4 q^2 - Am\omega^2)\Omega_W \\
&= \frac{\hbar^2}{8}A^2 m\omega^4 q^2\Omega_W - \frac{\hbar^2}{8}A\omega^2\Omega_W \ , \quad\quad\text{(C.16)}
\end{aligned}
$$

and

$$
\frac{\hbar^2}{8}m^2\omega^2\frac{\partial^2 \Omega_W}{\partial p^2} = \frac{\hbar^2}{8}m\omega^2\left(-\frac{A}{m}\Omega_W + A^2\frac{p^2}{m^2}\Omega_W\right)
$$

$$= -\frac{\hbar^2}{8}\omega^2 A\Omega_W + \frac{\hbar^2}{8}\omega^2 A^2 \frac{p^2}{m}\Omega_W \ . \qquad \text{(C.17)}$$

Dividing through by Ω_W, the Eq. (C.15) becomes

$$\begin{aligned}
-\frac{\partial A}{\partial \beta}H_W + \frac{\partial B}{\partial \beta} &= -\left(\frac{p^2}{2m} + \frac{1}{2}m\omega^2 q^2\right) + \frac{\hbar^2}{8}A^2 m\omega^4 q^2 - \frac{\hbar}{8}A\omega^2 \\
&\quad -\frac{\hbar^2}{8}\omega^2 A + \frac{\hbar^2}{8}\omega^2 A^2 \frac{p^2}{m} \\
&= -H_W + \frac{\hbar^2}{8}\left[A^2 m\omega^4 q^2 - A\omega^2 - \omega^2 A + \omega^2 A^2 \frac{p^2}{m}\right] \\
&= -H_W + \frac{\hbar^2}{4}\left[-A\omega^2 + \omega^2 A^2\left(\frac{1}{2}m\omega^2 q^2 + \frac{p^2}{2m}\right)\right] \\
&= -H_W + \left(\frac{\hbar\omega}{2}\right)^2\left[-A + A^2 H_W\right] \ . \qquad \text{(C.18)}
\end{aligned}$$

Thus

$$-\frac{\partial A}{\partial \beta}H_W + H_W = -\frac{\partial B}{\partial \beta} + \left(\frac{\hbar\omega}{2}\right)^2\left[-A + A^2 H_W\right] \ ,$$

and so

$$\left[-\frac{\partial A}{\partial \beta} + 1 - \left(\frac{\hbar\omega A}{2}\right)^2\right]H + \left[\frac{\partial B}{\partial \beta} + \left(\frac{\hbar\omega}{2}\right)^2 A\right] = 0 \ . \qquad \text{(C.19)}$$

All the terms in square brackets in Eq. (C.19) are independent of the phase-space coordinates q and p. Since this equation must hold for all values of (q, p), the two terms must vanish independently, and so

$$\frac{dA}{d\beta} - 1 + \frac{(\hbar\omega)^2}{4}A^2 = 0 \ , \qquad \text{(C.20)}$$

and

$$\frac{dB}{d\beta} + \frac{(\hbar\omega)^2}{4} A = 0 \ . \qquad \text{(C.21)}$$

Equation (C.20) can be rewritten

$$\frac{dA}{1 - \frac{(\hbar\omega)^2}{4} A^2} = d\beta \ . \qquad \text{(C.22)}$$

We now let $x = \frac{\hbar\omega}{2} A$. Then $dA = \frac{2}{\hbar\omega} dx$, and the above equation in terms of x is

$$\frac{2}{\hbar\omega} \int \frac{dx}{1 - x^2} \ = \ \int d\beta \ . \qquad \text{(C.23)}$$

Using the identity

$$\frac{1}{1 - x^2} = \frac{1}{2} \frac{d}{dx} \ln \left(\frac{1 + x}{1 - x} \right) \ , \qquad \text{(C.24)}$$

we get

$$
\begin{aligned}
\beta &= \frac{1}{\hbar\omega} \int dx \frac{d}{dx} \ln \left(\frac{1 + x}{1 - x} \right) \\
&= \frac{1}{\hbar\omega} \ln \left(\frac{1 + x}{1 - x} \right) \\
&= \frac{1}{\hbar\omega} \ln \left(\frac{1 + \frac{\hbar\omega}{2} A}{1 - \frac{\hbar\omega}{2} A} \right) \ .
\end{aligned}
\qquad \text{(C.25)}
$$

Or, written in exponential form:

$$e^{\hbar\omega\beta} = \frac{1 + \frac{\hbar\omega}{2} A}{1 - \frac{\hbar\omega}{2} A} \ .$$

Thus,

$$
\begin{aligned}
A &= \frac{2}{\hbar\omega}\frac{e^{\hbar\omega\beta}-1}{e^{\hbar\omega\beta}+1} \\
&= \frac{2}{\hbar\omega}\frac{e^{\frac{\hbar\omega}{2}\beta}-e^{-\frac{\hbar\omega}{2}\beta}}{e^{\frac{\hbar\omega}{2}\beta}+e^{-\frac{\hbar\omega}{2}\beta}} \\
&= \frac{2}{\hbar\omega}\tanh\left(\frac{\hbar\omega}{2}\beta\right) .
\end{aligned}
\tag{C.26}
$$

Substituting this result into Eq. (C.21) we obtain

$$
\frac{\partial B}{\partial\beta}+\left(\frac{\hbar\omega}{2}\right)\frac{2}{\hbar\omega}\tanh\left(\frac{\hbar\omega}{2}\beta\right)=0 .
\tag{C.27}
$$

The solution to (C.27) is

$$
B=-\frac{\hbar\omega}{2}\int d\beta\tanh\left(\frac{\hbar\omega\beta}{2}\right) .
\tag{C.28}
$$

To solve this integral, we consider

$$
\begin{aligned}
\tanh x &= \frac{\sinh x}{\cosh x} \\
&= \frac{d}{dx}\ln(\cosh x) .
\end{aligned}
\tag{C.29}
$$

Let $\frac{\hbar\omega\beta}{2}=x$, so $d\beta=\frac{2}{\hbar\omega}d\beta$. Then

$$
\begin{aligned}
B &= -\frac{\hbar\omega}{2}\frac{2}{\hbar\omega}\int dx\tanh x \\
&= -\int dx\frac{d}{dx}\ln\left(\cosh x\right) \\
&= -\ln\left(\cosh x\right)
\end{aligned}
$$

$$= -\ln\left[\cosh\left(\frac{\hbar\omega\beta}{2}\right)\right] . \tag{C.30}$$

We can now substitute this expression for B, as well as the expression for A given by Eq. (C.26), into the original ansatz Eq. (C.12) for the un-normalised distribution function:

$$\begin{aligned} \Omega_W &= e^{-AH_W+B} \\ &= e^{-\ln\cosh\left(\frac{\hbar\omega\beta}{2}\right)}e^{-\frac{2}{\hbar\omega}\tanh\left(\frac{\hbar\omega\beta}{2}\right)H} \\ &= \frac{1}{\cosh\left(\frac{\hbar\omega\beta}{2}\right)}e^{-\frac{2}{\hbar\omega}\tanh\left(\frac{\hbar\omega\beta}{2}\right)H} . \end{aligned} \tag{C.31}$$

To obtain the distribution function for the canonical ensemble, we now need to normalise Ω_W. The canonical partition function is defined as

$$\begin{aligned} Z(\beta) &= \int\int dqdp\,\Omega \\ &= \frac{1}{\cosh\left(\frac{\hbar\omega\beta}{2}\right)}\int\int dqdp\,e^{-\frac{2}{\hbar\omega}\tanh\left(\frac{\hbar\omega\beta}{2}\right)\left(\frac{p^2}{2m}+\frac{1}{2}m\omega^2q^2\right)} . \end{aligned} \tag{C.32}$$

This double integral factorises:

$$Z(\beta) = \frac{1}{\cosh\left(\frac{\hbar\omega\beta}{2}\right)}\int dp\,e^{-\frac{2}{\hbar\omega}\tanh\left(\frac{\hbar\omega\beta}{2}\right)\frac{p^2}{2m}}\int dq\,e^{-\frac{2}{\hbar\omega}\tanh\left(\frac{\hbar\omega\beta}{2}\right)\frac{m\omega^2}{2}q^2} . \tag{C.33}$$

Both integrals are simple Gaussians, and so

$$Z(\beta) = \frac{1}{\cosh\left(\frac{\hbar\omega\beta}{2}\right)}\left(\frac{\pi}{\left(\frac{1}{\hbar\omega m}\right)\tanh\left(\hbar\omega\beta\right)}\right)^{\frac{1}{2}}\left(\frac{\pi}{\left(\frac{m\omega}{\hbar}\right)\tanh\left(\hbar\omega\beta\right)}\right)^{\frac{1}{2}}$$

$$
\begin{aligned}
&= \frac{1}{\cosh\left(\frac{\hbar\omega\beta}{2}\right)} \frac{\pi}{\tanh\left(\frac{\hbar\omega\beta}{2}\right)} \frac{1}{\sqrt{\frac{1}{\hbar\omega m}\frac{m\omega}{\hbar}}} \\
&= \frac{\pi\hbar}{\cosh\left(\frac{\hbar\omega\beta}{2}\right)} \frac{\cosh\left(\frac{\hbar\omega\beta}{2}\right)}{\sinh\left(\frac{\hbar\omega\beta}{2}\right)} \\
&= \frac{\pi\hbar}{\sinh\left(\frac{\hbar\omega\beta}{2}\right)} \ .
\end{aligned} \tag{C.34}
$$

Now the Wigner transformed distribution function is given by

$$
\rho_W = \frac{1}{Z(\beta)}\Omega_W \ .
$$

Substituting the derived terms for $Z(\beta)$ and Ω_W yields the final result,

$$
\begin{aligned}
\rho_W(q,p,\beta) &= \frac{\sinh\left(\frac{\hbar\omega\beta}{2}\right)}{\pi\hbar} \frac{e^{-\frac{2}{\hbar\omega}\tanh\left(\frac{\hbar\omega\beta}{2}\right)H}}{\cosh\left(\frac{\hbar\omega\beta}{2}\right)} \\
&= \frac{1}{\pi\hbar}\tanh\left(\frac{\hbar\omega\beta}{2}\right) e^{-\frac{2}{\hbar\omega}\tanh\left(\frac{\hbar\omega\beta}{2}\right)H} \ .
\end{aligned} \tag{C.35}
$$

High-Temperature Limit

In the high-temperature limit, it is possible to show that we recover the classical canonical distribution function. We have

$$
T \to \infty, \quad \Rightarrow \beta \to 0 \ . \tag{C.36}
$$

We can write the hyperbolic tangent in terms of exponentials and take first-order approximations, so

$$
\begin{aligned}
\tanh\left(\frac{\hbar\omega\beta}{2}\right) &= \frac{e^{\frac{\hbar\omega\beta}{2}} - e^{\frac{\hbar\omega\beta}{2}}}{e^{\frac{\hbar\omega\beta}{2}} + e^{\frac{\hbar\omega\beta}{2}}} \\
&= \frac{1 + \frac{\hbar\omega\beta}{2} - \left(1 - \frac{\hbar\omega\beta}{2}\right)}{1 + \frac{\hbar\omega\beta}{2} + 1 - \frac{\hbar\omega\beta}{2}}
\end{aligned}
$$

$$= \frac{\hbar\omega\beta}{2} \ . \tag{C.37}$$

Then, Eq. (C.35) becomes

$$\begin{aligned}
\rho_W(q,p,\beta) &= \frac{1}{\pi\hbar}\frac{\hbar\omega\beta}{2}e^{\frac{2}{\hbar\omega}\frac{\hbar\omega\beta}{2}H_W} \\
&= \frac{\omega\beta}{2\pi}e^{-\beta H_W} \ . \tag{C.38}
\end{aligned}$$

The factor $\frac{\omega\beta}{2\pi}$ must be the inverse of the partition function for this to be the classical canonical result. This is easily checked:

$$\begin{aligned}
Z(\beta) &= \int\int dq dp\, e^{-\beta H} \\
&= \int dq\, e^{-\beta\frac{m\omega^2 q^2}{2}} \int dp\, e^{-\beta\frac{p^2}{2m}} \\
&= \sqrt{\frac{2\pi}{\beta m\omega^2}}\sqrt{\frac{2\pi m}{\beta}} \\
&= \frac{2\pi}{\beta\omega} \ . \tag{C.39}
\end{aligned}$$

We have thus shown that the classical canonical distribution function is recovered from the quantum-Wigner canonical distribution in the high-temperature limit.

Bibliography

[1] H. de Raedt, Lecture Notes, Como (1995).

[2] R. Kapral and G. Ciccotti, J. Chem. Phys. **110**, 8919-8929 (1999).

[3] S. Nielsen, R. Kapral and G. Ciccotti, J. Chem. Phys. **225**, 5805-5815 (2001).

[4] T. Beth and G. Leuchs, *Quantum Information Processing - Second Edition* (Wiley-VCH, Germany, 2005).

[5] D. G. Angelakis, M. Christandl, A. Ekert, A. Kay and S. Kulik, *Quantum Information Processing - From Theory to Experiment* (IOS Press, Amsterdam, 2006).

[6] G. Grynberg, A. Aspect and C. Fabre, *Introduction to Quantum Optics: From the Semi-classical Approach to Quantized Light* (Cambridge University Press, Cambridge, 2010).

[7] P. Kok and B. W. Lovett, *Introduction to Optical Quantum Information Processing* (Cambridge University Press, Cambridge, 2010).

[8] H. C. Öttinger, arXiv:1002.2938v1 [quant-ph] (2010).

[9] R. Kapral and G. Ciccotti, "Transport Coefficients of Quantum-Classical Systems", in *Computer Simulations in Condensed Matter: From Materials to Chemical Biology - Vol. 1*, M. Ferrario, G. Ciccotti and K. Binder Eds. (Springer, Berlin, 2006).

[10] A. Sergi and F. Petruccione, Phys. Rev. E **81**, 032101-1-032101-4 (2010).

[11] P. Pechukas, Phys. Rev. **181**, 166-174 (1969).

[12] P. Pechukas, Phys. Rev. **181**, 174-185 (1969).

[13] J. C. Tully and R. K. Preston, J. Chem. Phys. **55**, 562-573 (1971).

[14] W. H. Miller and F. F. George, J. Chem. Phys. **56**, 5637-5653 (1972).

[15] D. MacKernan, G. Ciccotti and R. Kapral, J. Chem. Phys. **116**, 2346-2353 (2002).

[16] E. J. Heller, B. Segev and A. V. Sergeev, J. Phys. Chem. B **106**, 8471-8478 (2002).

[17] I. V. Aleksandrov, Z. Natureforsch A, **36**, 902-908 (1981).

[18] V. I. Gerasimenko, Theor. Math. Phys. **50**, 77-87 (1982).

[19] W. Boucher and J. Traschen, Phys. Rev. D, **37**, 3522-3532 (1988).

[20] W. Y. Zhang and R. Balescu, J. Plasma Phys. **40**, 199-213 (1988).

[21] C. C. Martens and J. Y. Fang, J. Chem. Phys. **106**, 4918-4930 (1996).

[22] O. V. Prezhdo and V. V. Kisil, Phys. Rev. A **56**, 162-175 (1997).

[23] I. Horenko, C. Salzmann, B. Schmidt and C. Schutte, J. Chem. Phys. **117**, 11075-11088 (2002).

[24] Q. Shi and E. Geva, J. Chem. Phys. **121**, 3393-3404 (2004).

[25] D. A. Uken, A. Sergi and F. Petruccione, arXiv:1003.31172 [quant-ph] (2010).

[26] D. A. Uken and A. Sergi, "Momentum Shift in Nonadiabatic Dynamics", Submitted to Mod. Phys. Lett. B

[27] D. MacKernan, R. Kapral and G. Ciccotti, J. Phys.:Condens. Matter **14**, 9069-9076 (2002).

[28] See, for example, D. F. Styer *et al.*, Am. J. Phys. **70**, 288, 297 (2001).

[29] See, for example, R. Balescu, *Equilibrium and Non-equilibrium Statistical Mechanics* (John Wiley and Sons, New York, 1975).

[30] L. Landau and E. Lifshitz, *Quantum Mechanics - Non Relativistic Theory, 3rd Ed.* (Pergamon Press, London, 1977).

[31] W. B. Case, Am. J. Phys. **76**, 937-946 (2008).

[32] E. Wigner, Phys. Rev. **40**, 749-759 (1932).

[33] L. Ballentine, *Quantum Mechanics - A Modern Development* (World Scientific Publishing, 1998).

[34] A. Sergi, D. MacKernan, G. Ciccotti and R. Kapral, Theor. Chem. Acc. **110**, 49-58 (2003).

[35] A. Sergi, Phys. Rev. E **72**, 066125 (2005).

[36] A. Sergi and P. Giaquinta, Physics Essays **20** 629-639 (2007).

[37] A. Sergi, J. Phys. A: Math. Theor. **40**, F347-F354 (2007).

[38] J. McCauley, *Classical Mechanics* (Cambridge University Press, Cambridge, 1977).

[39] H. Goldstein, *Classical Mechanics, 2nd Ed* (Addison-Wesley, London, 1980).

[40] A. J. Leggett, S. Chakravarty, A. T. Dorsey, M. P. A. Fisher, A. Garg and W. Zwerger, Rev. Mod. Phys. **59**, 1-85 (1987).

[41] N. Makri and K. Thompson, J. Phys. Chem**291**, 101 (1998); K. Thompson and N. Makri, J. Chem. Phys. **100**, 1343-1353 (1999).

[42] A. Sergi, Atti. Acc. Pelor. Pericol. Cl. Sci. Fis. Mat. Nat. **87**, C1C0901001 (2009).

[43] G. S. Engel, T. R. Calhoun, E. L. Read, T. Ahn, T. Mančal, Y. Cheng, R. E. Blankenship and G. R, Fleming, Nature **446**, 782-786 (2007)

[44] D. Mac Kernan, G. Ciccotti and R. Kapral, J. Phys. Chem. B **112**, 424-432 (2008).

[45] M. Hillery, R. F. O'Connell, M. O. Scully and E. P. Wigner, Phys. Rep. **106**, 121-167 (1984)